Aus der Abteilung für Klinische Pharmakologie

Leiter: Prof. Dr. med. S. Endres

Medizinische Klinik Innenstadt

Klinikum der Universität

Ludwig-Maximilians-Universität München

Direktor: Prof. Dr. med. M. Reincke

Die Rolle des NLRP3-Inflammasoms in der Pathogenese entzündlicher Erkrankungen am Beispiel von Atherosklerose und der experimentellen Colitis

Dissertation

zum Erwerb des Doktorgrades der Humanbiologie

an der Medizinischen Fakultät der

Ludwig-Maximilians-Universität zu München

vorgelegt von

Peter Düwell

aus Oberstdorf

2011

Mit Genehmigung der Medizinischen Fakultät

der Universität München

1. Berichterstatter:	PD Dr. med. Max Schnurr
2. Berichterstatter:	apl. Prof. Dr. Stephan Brand
Mitberichterstatter:	Priv. Doz. Dr. Mario Müller
	Prof. Dr. Markus Sperandio
Mitbetreuung durch die promovierten Mitarbeiter:	Prof. Dr. med. Stefan Endres
	Dr. rer. biol. hum. Klaus Heckelsmiller
Dekan:	Prof. Dr. med. Dr. h. c. Maximilian Reiser, FACR, FRCR
Tag der mündlichen Prüfung:	09.05.2011

Meiner Familie und besonders meiner Oma Mayrock in Dankbarkeit

Inhaltsverzeichnis

1. Einleitung

Die Erkennung von mikrobiellen Infektionen und die Initiierung einer geeigneten Abwehr werden durch eine Vielzahl von Mechanismen des Immunsystems kontrolliert. Trifft das Immunsystem auf einen Krankheitserreger (Pathogen), so wird dieser zunächst von der angeborenen Immunabwehr erfasst (1), die sowohl zur Eliminierung des Erregers beiträgt als auch zur Etablierung der erworbenen, adaptiven Immunabwehr führt, vermittelt durch B- und T-Zellen. Das angeborene Immunsystem bildet somit die erste Linie der Abwehr und reagiert binnen weniger Minuten auf ein potenzielles Pathogen.

1.1 Angeborenes Immunsystem - *pattern recognition receptors* (PRRs)

Das angeborene Immunsystem besitzt die Fähigkeit zwischen „Selbst“ (z. B. eigene Proteine und Nukleinsäuren) und „Fremd“ (z. B. Mikroorganismen) zu unterscheiden (2-4). Dieses Dogma galt lange Zeit, dennoch stellte sich in den letzten Jahren zunehmend heraus, dass das Immunsystem Gefahrensignale *per se* erkennt. Hierbei kann es sich einerseits um exogene Pathogen- bzw. Mikroorganismus-assoziierte Strukturen (PAMP, *pathogen-associated molecular pattern*; MAMP, *microorganism-associated molecular pattern*), oder andererseits um endogene Moleküle handeln (DAMP, *danger-associated molecular pattern*). Hier sind deutlich Parallelen zu Matzinger´s „*Danger Hypothesis*“ zu erkennen, die ursprünglich für das adaptive Immunsystem beschrieben wurde (5). DAMPs wie z. B. das nukleäre Protein HMGB1, zytosolische DNA, 5’-Adenosintriphosphat und Harnsäurekristalle sowie PAMPs wie LPS, Flaggellin, RNA und unmethylierte DNA werden durch spezifische Rezeptoren, den so genannten *pattern recognition receptors* (PRRs) (6) erkannt. Diese PRRs umfassen eine Vielzahl an Erkennungsrezeptoren für verschiedenste endo- bzw. exogene Strukturmerkmale. Diese sind bei Zelltypen des Immunsystems, wie Monozyten, Makrophagen und dendritischen Zellen, aber auch bei epithelialen Zelltypen zu finden. Zu ihnen zählen Membranrezeptoren wie *Toll-like*-Rezeptoren (TLR) (7), zytosolische Helikasen wie *retinoic acid-inducible gene 1* (RIG-I)-*like* Rezeptoren (RIG-I, MDA-5, LGP-2) oder intrazelluläre Rezeptoren wie *nucleotide binding and oligomerization domain-like receptors* (NLRs)

(8). Damit steht eine maßgeschneiderte Immunabwehr zur Verfügung, die in der Lage ist, Motive verschiedensten Ursprungs zu erkennen.

Toll-like Rezeptoren

Die Bezeichnung *Toll-like*-Rezeptor leitet sich von einem Protein der Fruchtfliege Drosophila melanogaster ab, das vom einem Gen namens Toll codiert wird. Es wurde 1985 vom Team um Christiane Nüsslein-Volhard identifiziert (9). Es stellte sich heraus, dass Toll eine wichtige Funktion in der Abwehr gegen Pilzinfektionen hatte (10). TLRs spielen als PRRs eine wichtige Rolle. Sie erkennen konservierte, einfache Strukturen verschiedener Gruppen von Mikroorganismen und endogenen Proteinen. Auch in nicht-pathogenen, symbiontischen Mikroorganismen sind diese Strukturen zu finden. Während „nicht-signalisierende" PRRs wie Akute-Phase-Proteine an eindringende Mikroorganismen binden, um nachfolgende Phagozytose zu erleichtern, handelt es sich bei TLRs um signalisierende, transmembrane PRRs. Mit der Identifizierung molekularer, mikrobieller Komponenten war eine Unterteilung in Lipide, Polysaccharide, Proteine und Nukleinsäuren möglich. Bislang sind in Säugetieren zwölf verschiedene TLRs Identifiziert (4, 11-13). TLR1, TLR2, TLR4, TLR5, TLR6 und TLR11 (nur in der Maus) sind in der Zellmembran verankert und TLR3, TLR7, TLR8 und TLR9 sind in intrazellulären Vesikeln bzw. dem endoplasmatischen Retikulum zu finden. TLR-Liganden Erkennung führt neben der Aktivierung von MAP-Kinasen (MAPK, *mitogen-activated protein kinases*) zur Translokation von Transkriptionsfaktoren wie NF-κB (*nuclear factor-κB*) und *interferon regulatory factor* (IRF) 3 und 7. Die extrazelluläre Domäne, *LRR-domain (leucine rich repeats)*, dient der Ligandenbindung, während die intrazelluläre Domäne, TIR-Domäne (*Toll-IL-1 receptor homologous domain*), zur Signalweiterleitung führt. Mit Ausnahme von TLR3 haben alle Rezeptoren gemeinsam, dass sie über das Adapterprotein MyD88 (*myeloid differentiation primary response gene 88*) mit IRAK (*IL-1 receptor-associated kinase*) assoziieren und somit zur Translokation von IRFs und NF-κB führen. TLR3 hingegen, bindet an TRIF (*TIR-domain-containing adapter-inducing interferon-β*). IRFs und NF-κB initiieren die Transkription von proinflammatorischen Zytokinen IL-1β, IL-6, IL-12p40 und TNF-α sowie von Typ-I-Interferonen (IFN-α und β). Die weite Verbreitung von TLRs nicht bei von Immunzellen des angeborenen sondern auch bei Zellen des

adaptiven Immunsystems (B- und T-Zellen), machen diese zu einem exzellenten Werkzeug, mit dessen Hilfe angeborenes und erworbenes Immunsystem übergreifend für die Erkennung als Grundlage zur Elimination von Pathogenen sorgen.

Zytosolische *pattern-recognition*-Rezeptoren

Zusätzlich zum TLR-System, welches PAMPs auf der Zelloberfläche bzw. in Vesikeln erkennt, wurden kürzlich auch zytoplasmatische PRRs beschrieben. Die Entdeckung dieser Rezeptoren beruhte auf der Annahme, dass intrazellulär eingedrungene Pathogene nicht über membrangebundene Rezeptoren erfasst werden können, um eine Immunreaktion auszulösen. Zu diesen zytosolischen Rezeptorfamilien zählen die *retinoic acid-inducible gene I* (RIG-I)*-like receptors* (RLRs) und die *nucleotide-binding oligomerization domain like receptors* (NLRs).

Retinoic acid-inducible gene I-like receptors

Zu dieser Familie gehören die zytosolischen Helikasen *retinoic acid-inducible gene I* (RIG-I), *melanoma differentiation-associated gene 5* (MDA-5) und *laboratory of genetics and physiology 2* (LGP-2). Sie erkennen virale RNA im Zytoplasma (11, 14). Durch extensive Forschung an Mäusen mit entsprechenden Gendefekten für die einzelnen Rezeptoren konnte ihnen die Erkennung verschiedener Viren zugeordnet werden (15, 16). RIG-I erkennt einzelsträngige und doppelsträngige RNA u. a. von Influenza A, *vesicular stomatitis virus* und Japanischem Enzephalitis-Virus. Entscheidend hierfür sind bestimmte Strukturen der RNA sowie eine Triphosphat-Gruppe am 5´-Ende (17, 18). Erwähnenswert ist hierbei die Unterscheidung zwischen „Selbst"- und „Fremd"-RNA, da eigene RNA im Zytoplasma der Zelle nicht mit einer freien Triphosphat-Gruppe auftritt. Diese wird entweder mittels 5´-Capping (modifiziertes Guanosin) oder über RNA-Nukleosidmodifikationen geschützt. MDA-5 erkennt RNA von Enzephalomyokarditis-Virus (EMCV), Mengo bzw. Theiler´s Viren (19). Ein synthetischer Ligand für MDA-5 ist poly(I:C) (polyinosinic:polycytidylic acid) (16, 20). Sowohl RIG-I als auch MDA-5 besitzen eine N-terminale CARD (*caspase recruitment domain*) und eine Helikase-Domäne, RIG-I zusätzlich eine *C-terminal repressor domain* (CRD). Während die Helikase-Domäne und die CR-Domäne RNA binden,

dient CARD für die Signalweiterleitung via CARD-CARD Interaktionen (Adaptermoleküle bzw. Proteine mit CARD). Nach Bindung an das Adapterprotein MAVS (alternative Namen sind IPS-1, VISA oder Cardif), führt die Signalkaskade über TRADD (*tumor necrosis factor receptor type 1-associated DEATH domain*) zur Translokation der Transkriptionsfaktoren NF-κB bzw. IRF3 und IRF7 mit Induktion von Typ-I-Interferonen. Die Funktion von LGP-2 ist weitgehend unbekannt. Es wird vermutet, dass LGP-2 an RIG-I bindet und eine inhibitorische Funktion ausübt (14).

Nucleotide-binding oligomerization domain* (*NOD)-like receptors

Eine zweite wichtige Rezeptorfamilie bilden die NOD-*like*-Rezeptoren. Diese bestehen aus einer N-terminalen Effektordomäne (CARD, Pyrin oder BIR), einer zentralen *nucleotide oligomerization domain* (NOD) und C-terminalen *leucine rich repeats* (LRR). Die N-terminale Effektordomäne dient der Signalweiterleitung via Protein-Protein-Interaktionen und die C-terminale LRRs sind meist die Erkennungsregionen von PAMPs (21, 22). Von diesen Rezeptoren sind mindestens 23 humane und 34 murine Typen bekannt, deren physiologische Eigenschaften noch wenig erforscht sind (23, 24). NLRs können wiederum in mindestens fünf Unterkategorien eingeteilt werden; NLRA (*acidic transactivation domain*), NLRB (*baculovirus inhibitor of apoptosis protein repeat* – BIR), NLRC (*CARD domain*), NLRP (*pyrin domain*) und NLRX, dessen Bestandteile unbekannt sind (25, 26). Diese Rezeptoren können eine Vielzahl an intrazellulären PAMPs, wie Motive bakteriellen Ursprungs oder virale DNA detektieren (27). Durch Ligandenbindung werden verschiedene Signalwege aktiviert, z. B. über *mitogen-activated protein kinases* (MAPK) zur Translokation von NF-κB und Transkription proinflammatorischer Zytokine oder Typ-I-Interferone.

1.2 Das Inflammasom

Einige NLRs können multimere Komplexe formen, so genannte Inflammasome (28). Durch ihre Formierung und Aktivierung wird die Protease Caspase-1 (*cysteinyl-aspartate specific protease,* auch *interleukin 1 converting enzyme* genannt) rekrutiert, die für die Spaltung von Zytokinen der IL-1 Familie in deren

bioaktive Formen verantwortlich ist. Inflammasome sind zytosolische Proteinkomplexe, die vorwiegend in Immunzellen wie dendritischen Zellen und Makrophagen vorkommen. Sie können, je nach Interaktionspartner, in vier Gruppen unterteilt werden; das NLRP1-, das NLRP3-, das NLRC4 (IPAF)- und das AIM-2-Inflammasom (Abbildung 1).

Durch Bindung an das Adaptermolekül ASC (*apoptosis-associated speck-like protein*) kann Caspase-1 gebunden und aktiviert werden.

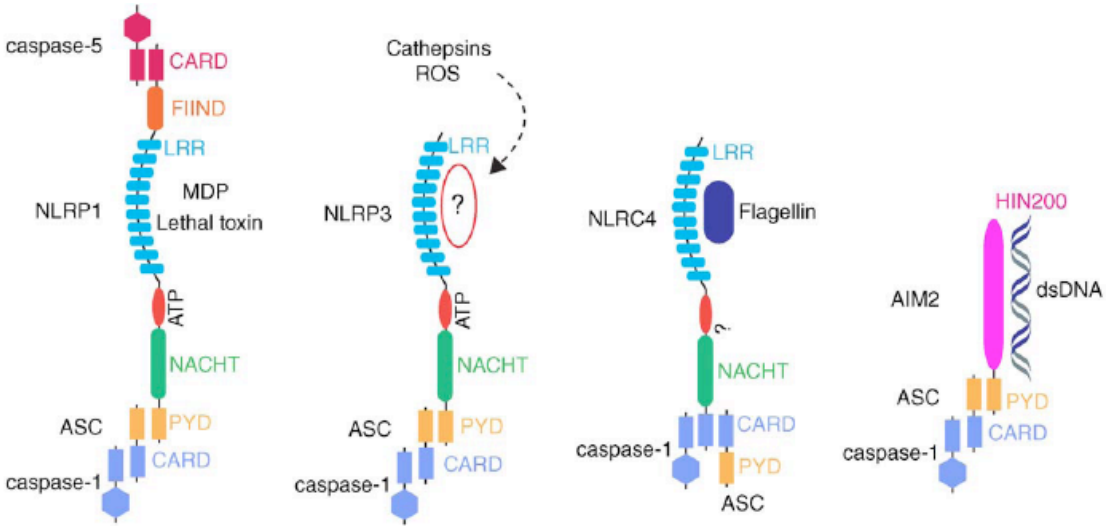

Abbildung 1: Schematische Darstellung verschiedener Inflammasome mit putativen Liganden oder Aktivatoren. Je nach Bindungspartner wird über das Adaptermolekül ASC Caspase-1 rekrutiert und es entsteht der Inflammasom-Komplex. Schema nach Latz E., et al. (29).

PAMPs wie Muramyldipeptid (MDP) und *anthrax lethal toxin* werden über NLRP1 (30, 31) und Bakterien wie Salmonellen, Legionellen, Shigellen und Pseudomonaden durch IPAF erkannt (32). Von den verschiedenen Inflammasomen ist das NLRP3-Inflammasom am besten charakterisiert. NLRP3 wird durch eine Vielzahl von Bakterien (u. a. Staphylokokken, Listerien oder Neisseria), Viren (u. a. EMCV, Sendai- und Influenza-Viren) und Pilzen (u. a. Candida und Saccharomyces) aktiviert (33-36) (Tabelle 1). Eine wichtige Entdeckung waren jedoch endogene Faktoren zellulären Stresses, die zur Aktivierung von NLRP3 führen (extrazellulär freigesetztes ATP, Hyaluronan oder Amyloid-β) (34, 37, 38). Eine weitere Klasse von potenziellen NLRP3-Stimuli bilden Moleküle metabolischen Stresses wie Harnsäurekristalle (Gicht) und Cholesterinkristalle (Atherosklerose) (39, 40) oder Umwelt-Reizstoffe wie Siliziumoxid, Asbest und UV-B-Strahlung (41-44).

PAMP-enthaltende Mikroorganismen		
Viren	Adenovirus	(36)
	Influenza Virus	(35, 45)
	Enzephalomyocarditis Virus	(46)
	Sendai Virus	(35)
Bakterien/ Toxine	Listeria monocytogenes	(34)
	Neisseria gonorrhoeae	(47)
	Staphylococcus aureus	(34)
	Toxine	(34, 48, 49)
Pilze	Candida albicans	(33)
	Saccharomyces cerevisiae	(33)
DAMPS		
Kristalle	Aluminiumhydroxid	(41, 50-53)
	Asbest	(42, 43)
	Cholesterin	(40)
	Harnsäure	(39)
	Siliziumdioxid	(41-43)
Sonstige	Amyloid-β	(38)
	ATP	(34)
	Glucose	(54)
	Hyaluronan	(37)
	Imidazochinoline	(35)

Tabelle 1: Liganden bzw. Stimuli des NLRP3-Inflammasoms. Modifiziert nach Schroder K., et al. (55).

Die Mechanismen, die zur Aktivierung des NLRP3-Inflammasoms führen, sind noch nicht vollständig geklärt. Es werden drei Modelle diskutiert (Abbildung 2). Das erste Modell propagiert, dass extrazelluläres ATP zur Bildung von Pannexin-1 Membranporen führt. Durch den daraus entstehenden intrazellulären Kalium-Verlust wird NLRP3 rekrutiert und einströmende, potenzielle Stimuli können NLRP3 direkt aktivieren (56). In einem zweiten Modell führen partikuläre Substanzen die via Endozytose aufgenommen wurden zur Zerstörung der Endo-Lysosomen. Die Freisetzung von lysosomalen Bestandteilen (z. B. Cathepsine) aktivieren auf bisher unbekannte Weise NLRP3 (38, 41). Im dritten Modell werden reaktive Sauerstoff Spezies (ROS) für die Aktivierung von NLRP3 verantwortlich gemacht (42, 43, 57). In allen Modellen sind für die Aktivierung des NLRP3 Inflammasoms zwei Signale notwendig. Im ersten Schritt werden über transkriptionellem Weg (über TLRs oder NLRs) die Expression der inaktiven pro-Form von IL-1β sowie NLRP3 selbst reguliert

(58). In einem zweiten Schritt entsteht durch oben genannte Modelle der NLRP3 Inflammasom-Komplex. Dabei dimerisieren oder multimerisieren die Pyrin-Domänen von NLRP3 und ASC bzw. die CARD-Domänen von ASC und Caspase-1 wobei die katalytisch aktive Caspase-1 entsteht und im folgenden Prozess pro-IL-1β in seine biologisch aktive Form überführt (Abbildung 1). IL-1β wiederum ist das Hauptzytokin für inflammatorische Immunreaktionen, Fieber und metabolische Erkrankungen.

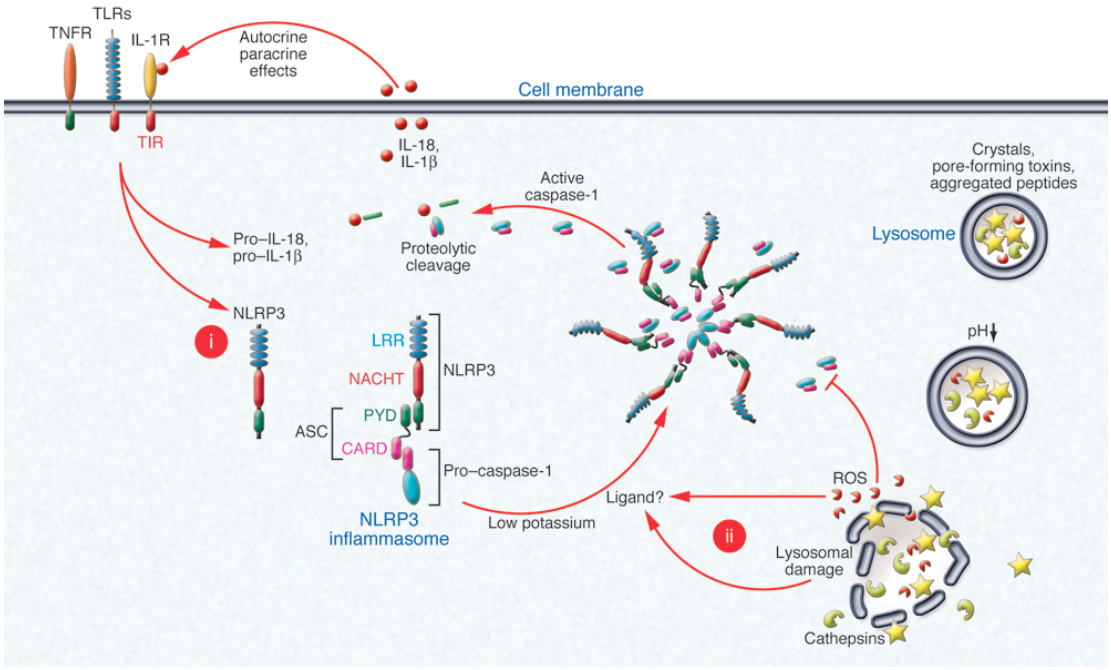

Abbildung 2: Diskutierte Modelle zur Aktivierung des NLRP3 Inflammasoms. Der erste Schritt (i) reguliert auf transkriptionellem Weg die Expression von pro-IL-1β bzw. IL-18 sowie von NLRP3 selbst. Im zweiten Schritt (ii) entstehen die bioaktiven Formen von IL-1β und IL-18 durch Aktivierung des NLRP3-Inflammasom-Komplexes (Kaliumverlust, endo-lysosomale Destabilisierung, ROS). Schema nach Stutz A., et al. (59).

1.3 NLRP3-Inflammasom-assoziierte Erkrankungen

Das angeborene Immunsystem besitzt mit den TLRs und den NLRs zwei Erkennungssysteme zur schnellen und unspezifischen Abwehr von Pathogenen (PAMPs). Dennoch stellte sich sehr schnell heraus, dass die Bindung von nicht-mikrobiellen Gefahrenmolekülen (DAMPs) eine ebenso heftige Immunreaktion auslösen kann, was zu einer Freisetzung von Entzündungsmediatoren wie IL-1β und IL-18 führt. Dabei kann es sich um DAMPs wie extrazelluläres ATP (aus zerstörten

oder aktivierten Zellen), kristalline Strukturen (Asbest, Siliziumoxid, Harnsäure-, Kalziumpyrophosphat- oder Cholesterinkristalle) oder reaktive Sauerstoff-Spezies (ROS) handeln. Allen Substanzen ist gemein, dass diese zur NLRP3-Aktivierung führen und somit die Freisetzung von IL-1β veranlassen. Nachdem IL-1β in bioaktiver Form freigesetzt wurde, bindet es an seinen Rezeptor (IL-1R) und initiiert Entzündungsreaktionen verschiedener Art (60). Eine fehlgeleitete Aktivierung des NLRP3-Inflammasoms wurde mit diversen Erkrankung in Verbindung bebracht, auf die hier in Kürze eingegangen werden soll.

NLRP3-Mutationen

Einige erblich-bedingte oder erst im Lebensverlauf auftretende Erkrankungen stehen im Zusammenhang mit erhöhten IL-1β-Serumspiegeln (60). Heute bereits werden mehrere dieser Krankheiten erfolgreich mit IL-1-Antagonisten behandelt. Viel versprechend ist Anakinra, ein rekombinantes Analogon zum natürlich vorkommenden IL-1-Rezeptor-Antagonisten (IL-1RA). Wie bereits erwähnt, spielt das NLRP3-Inflammasom eine wichtige Rolle bei der Freisetzung von bioaktivem IL-1β. Mutationen im NLRP3-Gen konnten als Auslöser seltener, entzündlicher Autoimmunkrankheiten identifiziert werden. Diese Autoimmunkrankheiten werden unter dem Überbegriff c*ryopyrin-associated-periodic syndromes* (CAPS) zusammengefasst. Dabei handelt es sich um periodisch auftretende Fieber- und Entzündungsschübe. Neben CINCA (c*hronic infantile cutaneous neurological articular syndrome*) sind außerdem FCAS (f*amilial cold autoinflammatory syndrome*) und MWS (*Muckle-Wells syndrome*) bekannt. Bei Letzteren liegt die Ursache in einer Überaktivität von NLRP3 mit daraus resultierenden, hohen IL-1β-Spiegeln (61, 62). Die Erkenntnis der molekularen Grundlage dieser Erkrankungen haben die klinischen Behandlungsmöglichkeiten von Grund auf verändert.

Gicht und Pseudogicht

In den letzten Jahren konnten Gicht bzw. Pseudogicht mit NLRP3 in Verbindung gebracht werden (39). In beiden Erkrankungen, denen jedoch ein unterschiedlicher

Pathomechanismus zugrunde liegt, ist die Entzündungsursache eine erhöhte Bildung und Ausfällung von Harnsäure- bzw. Kalziumpyrophosphatkristalle in den Gelenken. Eine Vermutung bezüglich der bevorzugten Kristallbildung liegt in der niedrigeren Temperatur in den Gelenken und der damit verbundenen geringeren Löslichkeit der Kristalle. Diese Kristalle sind ein starker Aktivator von NLRP3 und verursachen eine ausgeprägte Freisetzung von IL-1β. Dieser pathophysiologische Zusammenhang konnte auch in klinischen Studien belegt werden, in denen Antagonisten von IL-1β erfolgreich eingesetzt wurden (63-66).

Silikose/Asbestose

Eine Gefahr für die Gesundheit geht auch von anderen kristallinen Substanzen, nämlich Silizium- und Asbeststaub aus. Beruflich bedingte Inhalation von diesen kristallinen Stoffen kann zu Lungenfibrose bis hin zu Lungen- und Pleurakrebs führen (67). Die Aufnahme dieser Stoffe durch Alveolarmakrophagen führt NLRP3-abhängig zur vermehrten Produktion von IL-1β (43). Ähnliche Entzündungsreaktionen konnten auch für partikuläre Substanzen wie Dieselrußpartikel oder Zigarettenrauch gefunden werden (68, 69). Somit vermitteln NLRP3-abhängige chronische Entzündungsprozesse, Lungengerüsterkrankungen und wahrscheinlich auch Krebs.

Morbus Alzheimer

Morbus Alzheimer ist eine fortschreitende, neurodegenerative Erkrankung der Gehirnnerven durch Ablagerung von meist falsch gefalteten β-Amyloid-Peptidketten (Alzheimer-Plaques) im zentralen Nervensystem (70, 71). Die Folgen sind zunehmende Verschlechterung der kognitiven Leistungsfähigkeit und neuropsychologische Störungen. Phagozytierende Zellen im Zentralnervensystem (Mikroglia) werden durch β-Amyloid-haltige Plaques zur Phagozytose angeregt und schütten inflammatorische Zytokine aus (71-73). Erhöhte IL-1β-Spiegel wurden sowohl beim Menschen mit Morbus Alzheimer als auch in entsprechenden Mausmodellen gefunden (72, 74) und konnten mit einer β-Amyloid-abhängigen NLRP3-Aktivierung in Verbindung gebracht werden (38). Somit spielen

NLRP3-vermittelte Entzündungsprozesse auch bei neurodegenerativen Erkrankungen eine pathogenetische Rolle.

Andere NLRP3-assoziierte Krankheiten

Kontakt-Hypersensitivität ist eine allergische Reaktion vom Typ 4 (Spättyp). Dieser Typ ist mit einer Aktivierung von IL-1β und IL-18 durch das NLRP3-Inflammasom in Verbindung gebracht worden. Ein Beispiel hierfür ist das Kontaktallergen 2,4-Trinitrochlorbenzol (75).

Diabetes mellitus Typ 2 ist eine Stoffwechselerkrankung mit erhöhten Blutzuckerwerten (Hyperglykämie) und Insulinresistenz, die durch Übergewicht sowie durch genetische Prädisposition entstehen kann. Vor einigen Jahren konnte IL-1β als Risikofaktor für die Erkrankung an Typ 2 Diabetes identifiziert werden (76). Hierbei führen erhöhte IL-1-Spiegel zur Insulinresistenz, Zerstörung insulinproduzierender β-Inselzellen und konsekutiv zur Hyperglykämie (77). Die erhöhten extrazellulären Glucosespiegel scheinen Auslöser für eine bisher ungeklärte, NLRP3-abhängige Freisetzung von bioaktivem IL-1β zu sein (78).

1.4 Zusammenfassung der präsentierten Arbeiten

Das angeborene Immunsystem besitzt eine Vielzahl an Erkennungsmechanismen für pathogene Strukturen, um eine maßgeschneiderte Abwehr gegen Gefahrensignale mikrobiellen, aber auch körpereigenen Ursprungs zu bilden. Eine besondere Rolle spielt das NLRP3-Inflammasom, welches diverse, pathophysiologisch vollständig unterschiedliche Erkrankungen, wie erblich bedingte Autoimmunkrankheiten, Stoffwechselerkrankungen (Gicht, Pseudogicht, Diabetes mellitus Typ 2), neurodegenerative Erkrankungen (Morbus Alzheimer), chronisch fibrosierende Lungenerkrankungen (Silikose und Asbestose) und möglicherweise sogar Krebserkrankungen (Bronchialkarzinom, Pleuramesotheliom) vermittelt. Die jeweiligen pathophysiologischen Mechanismen, die zur Aktivierung bzw. Fehlregulation des Inflammasoms führen, sind jedoch nur unvollständig aufgeklärt.

Ein besseres Verständnis dieser Mechanismen kann daher zu einer zielgerichteten Therapie akuter und chronischer Erkrankungen beitragen.

Der erste Teil meiner Arbeit beschäftigt sich mit einer Theorie zur NLRP3-Aktivierung im Zusammenhang mit der Entstehung von Atherosklerose. Die Atherosklerose ist eine Systemkrankheit, die, begünstigt durch genetische Faktoren, im Laufe von Jahren zu Veränderungen von Gefäßwänden mit das Lumen einengenden Ablagerungen führt. Diese Ablagerungen (auch Plaques genannt) enthalten große Mengen an Cholesterin, das im Normalfall über HDL aufgenommen und zur Leber transportiert und abgebaut wird. Cholesterin ist ein wichtiger Bestandteil von Zellmembranen und wird vermutlich bei Überangebot mit Hilfe der A:Cholesterin-Acyltransferase (ACAT) als Ester (lösliche Form) gespeichert. Die inflammatorische Natur von Atherosklerose ist seit langem bekannt. Übersteigt die Menge an freiem Cholesterin die Aufnahmekapazität der Zellen, werden Makrophagen angelockt und versuchen dann dieses aufzunehmen und abzubauen. Makrophagen sind aber nicht in der Lage, Kristallstrukturen abzubauen. Es entsteht eine sich selbst unterhaltende Entzündungsreaktion mit zunehmender Plaquelast. In atherosklerotischen Plaques konnten in histologischen Untersuchungen Aussparungen gefunden werden, die von Cholesterinkristallen verursacht wurden (sog. *crystal clefts*) und im Rahmen der histologischen Aufarbeitung durch organische Lösungsmittel herausgelöst wurden. Es ist jedoch weitgehend unbekannt, ob Cholesterinkristalle bereits bei der Entstehung von Atherosklerose eine wichtige Rolle spielen und ob diese für die Entzündungsreaktion verantwortlich sind.

In einem Apo-E-transgenen Mausmodell, in dem mit einer Cholesterin-reichen Nahrung eine beschleunigte Atherosklerose induziert wird, konnten wir zeigen, dass kleinste Cholesterinkristalle bereits nach zwei Wochen in den Plaques großer Gefäße nachweisbar waren. Ebenso konnten Immunzellen identifiziert werden, die sich um diese Kristalle ansammelten. Nachdem bekannt war, dass verschiedene Kristalle in der Lage sind, eine NLRP3-Inflammasom-vermittelte Entzündungsreaktion hervorzurufen, waren wir daran interessiert, ob Cholesterinkristalle eine ähnliche Eigenschaft besitzen. Tatsächlich zeigten *in vitro* Versuche mit Makrophagen-Zelllinien eine IL-1β-Sekretion nach Inkubation mit Cholesterinkristallen. Diese blieb bei Makrophagen mit NLRP3-, ASC- oder Caspase-1-Defizienz aus. Zudem konnte die Beteiligung von Cathepsinen an der NLRP3-Aktivierung nachgewiesen werden, die mechanistisch auf eine

Destabilisierung des Phagolysosoms hinweisen. In einem weiteren Mausmodell wurden schließlich Knochenmarkszellen von Wildtyp bzw. von Tieren mit Defizienz in verschiedenen NLRP3-Inflammasom-Komponenten in LDL-Rezeptor-defiziente Mäuse transferiert und das Auftreten atherosklerotischer Plaques erfasst. Es zeigte sich eine deutlich abgemilderte Form von Atherosklerose in Tieren, die mit Knochenmark von Mäusen mit Defekten in der NLRP3-Inflammasom-Aktivierung rekonstituiert wurden.

Zusammenfassend zeigt diese Studie, dass bereits in der Frühform der Atherosklerose mikrokristallines Cholesterin vorhanden ist und dieses mutmaßlich, vermittelt über Komponenten der NLRP3-Inflammasom-Kaskade, zur Entstehung und Progression von Atherosklerose beiträgt. Somit stehen potenziell neue Therapieansätze für Atherosklerose und deren Folgeerkrankungen, die in der westlichen Welt für die meisten Todesfälle verantwortlich sind, zur Verfügung.

Im zweiten Teil meiner Arbeit wurde der Einfluss des NLRP3-Inflammasoms auf die Entstehung chronisch entzündlicher Darmerkrankungen anhand eines murinen Colitismodells untersucht, welches in vielen Studien herangezogen wird, um deren Entstehung, Progression und Therapie zu erforschen. Der Morbus Crohn und die Colitis ulcerosa sind chronisch entzündliche Darmerkrankungen, deren Pathogenese nicht vollständig geklärt ist. Es wird von Beteiligung genetischer sowie umweltbedingter Faktoren ausgegangen. Interessanterweise stehen Polymorphismen des NLRP3-Gens mit einer erhöhten Anfälligkeit für Morbus Crohn in Zusammenhang (79). Ein wichtiger Befund bei diesen Erkrankungen sind erhöhte Spiegel von Entzündungsmediatoren wie IL-1β und TNF-α. Mit dem DSS (*dextran sulfate sodium*)-Colitismodell, in dem die Tiere den sulfatierten Makrozucker DSS im Trinkwasser erhalten, steht ein Modell zur Verfügung, das eine klinische Symptomatik ähnlich der akuten Kolitis aufweist. Die Tatsache, dass erhöhte Mengen an IL-1β im DSS-Colitismodell detektierbar sind und Caspase-1-Inhibitoren einen therapeutischen Effekt aufweisen (80), ließen eine Beteiligung des NLRP3 Inflammasoms vermuten.

Tatsächlich stellte sich heraus, dass mit DSS inkubierte Makrophagen *in vitro* dosisabhängig IL-1β sezernieren. Dieses Phänomen war von der Molekülintegrität abhängig, was darauf schließen lässt, dass das Makromolekül an sich für die Aktivität verantwortlich ist. Makrophagen-Zelllinien mit Defekten in NLRP3, ASC oder Caspase-1 zeigten schließlich ein nahezu vollständiges Fehlen der IL-1β–Freisetzung. Für die Freisetzung von IL-1β war eine vorhergehende

Aktivierung der Makrophagen mit LPS (Signal 1) erforderlich. Im *in vivo* Colitisversuch mit DSS im Trinkwasser zeigten NLRP3-defiziente Mäuse im Gegensatz zu Wildtyp-Mäusen über einen Zeitraum von neun Tagen eine signifikant geringer ausgeprägte Kolitis (weniger Durchfälle und Blut im Stuhl). Dieser Befund korrelierte mit einer geringeren Menge an proinflammatorischen Zytokinen im Darmgewebe sowie weniger ausgeprägten entzündlichen Veränderungen in der Histologie. Diese Befunde deuten auf eine Beteiligung des NLRP3-Inflammasoms in der Entzündungsreaktion bei der DSS-induzierten Colitis hin.

Zusammenfassend lassen sich diese Befunde in einem Zwei-Phasen-Modell beschreiben: In einem ersten Schritt, vermittelt durch toxische Effekte von DSS auf die Epithelbarriere des Darms, treffen (physiologisch) vorhandene Darmbakterien auf Makrophagen in der Darmmukosa, was über Rezeptoren des angeborenen Immunsystems die Transkription von pro-IL-1β bewirkt. Im zweiten Schritt kommt es zu einer Aktivierung des NLRP3 Inflammasoms mit Freisetzung von bioaktivem IL-1β, welches ein Schlüssel-Zytokin für die Initiation und Progression entzündlicher Prozesse ist.

1.5 Summary of presented publications

Innate immunity covers a multiplicity of recognition mechanisms for pathogens to ensure a customized defense against microbial and endogenous danger signals. In this regard, the NLRP3 inflammasome plays a major role arranging diverse and pathophysiologically completely different diseases such as congenital autoimmune diseases, metabolic diseases (gout, pseudo-gout and type 2 diabetes), neurodegenerative diseases (Alzheimer disease), chronic fibrosing lung disease (silicosis, asbestosis) and possibly cancer (bronchial carcinoma, pleura mesothelioma). The distinct pathophysiological mechanisms that lead to the activation or dysregulation of the inflammasome are incompletely elucidated. A better comprehension of these mechanisms may contribute to novel therapies of acute and chronic diseases.

The first part of my work engages in a theory of NLRP3 activation in connection with the development of atherosclerosis. Atherosclerosis is a systemic disease that over the years, fostered by genetic factors, leads to changes of vascular walls including

confining deposit. This deposit (also called plaque) contains huge amounts of cholesterol that is normally absorbed by HDL and transported to the liver for degradation. Cholesterol is a crucial component of cell membranes and at excessive supply it is suggested to be stored as an ester (soluble form) mediated by A:cholesterol acyltransferase (ACAT). The inflammatory property of cholesterol has been known for a long time. If the amount of free cholesterol exceeds the uptake capacity of cells, macrophages get attracted and try to absorb and degrade the cholesterol. However, macrophages are not capable of degrading crystalline structures. A self-entertaining inflammatory response with increasing plaque burden occurs. Histological examinations of late atherosclerotic lesions show cavities caused by cholesterol crystals (so called crystal clefts) which occur during histological procedures with organic solvents. However, it remains unknown if cholesterol crystals occur already in early atherosclerotic lesions and whether these are responsible for triggering the inflammatory response.

Inducing accelerated atherosclerosis with a high-cholesterol diet in an Apo-E transgenic mouse model, we could show that minute amounts of cholesterol crystals were present in lesions after only two weeks of diet. We also could identify immune cells accumulating around these crystals. Because it was known that different crystals have the ability to induce NLRP3-dependent inflammation, we were interested if cholesterol crystals have similar properties. In deed, *in vitro* experiments with macrophage cell lines showed IL-1β secretion after incubation with cholesterol crystals. This was not the case for macrophages with NLRP3-, ASC- or caspase-1-deficiency. In addition, involvement of cathepsins could be verified suggesting phago-lysosomal rupture. In an additional mouse model using lethally irradiated LDLR-deficient donor mice that have been reconstituted with bone marrow from mice lacking different NLRP3 inflammasome components, we measured the appearance of atherosclerotic lesions. Mice that had been reconstituted with bone marrow of NLRP3 inflammasome components showed a significantly ameliorated form of atherosclerosis.

In summary, this study shows that even at an early stage of disease, minute amounts of crystalline cholesterol are present, and that it presumably contributes to the development and progression of atherosclerosis, mediated by components of the NLRP3 inflammasome. These insights open a new field for pharmacological research developing novel therapeutic strategies for the treatment of atherosclerosis and its sequelae that are responsible for most fatalities in the Western world.

The second part of my work focuses on the impact of the NLRP3 inflammasome on the development of inflammatory bowel disease (IBD). The studies were performed in a murine colitis model that has frequently been used to explore the pathogenesis, progression and therapy of IBD.

Crohn´s disease and ulcerative colitis are two forms of inflammatory bowel disease with as yet incompletely clarified pathogenesis. The involvement of genetic and environmental factors is being discussed. Interestingly, polymorphisms of the NLRP3 gen are associated with a higher susceptibility to Crohn´s disease (79). Important findings in these diseases are elevated levels of inflammatory mediators such as IL-1β and TNF-α. The DSS (dextransulfate sodium) colitis model, in which mice receive the sulfated macro sugar DSS in drinking water, is a valuable model mirroring many features of acute colitis observed in humans. Elevated levels of IL-1β as well as therapeutic efficacy of caspase-1 inhibitors suggest an involvement of the NLRP3 inflammasome in this model.

In fact, macrophages incubated with DSS secrete IL-1β in a dose dependent manner. This phenomenon was dependent on the molecule integrity assuming that the whole molecule is responsible for the activity. Macrophage cell lines with defects in NLRP3, ASC or caspase-1 showed an almost complete failure of IL-1β release. However, prior activation with LPS (signal 1) was essential for the release of IL-1β. In the DSS colitis model, NLRP3-deficient mice showed a significantly less severe colitis (less diarrhea and bloody feces) compared to wild type mice during a period of nine-days. This finding correlated with a reduced level of inflammatory cytokines in the colon epithelium as well as less severe histological changes. These results point at an involvement of the NLRP3 inflammasome in DSS-induced colitis.

In summary, these results support a two-phase model: In the first step, mediated by the toxic effects of DSS on the colon epithelium, (physiologically) existing intestinal bacteria encounter mucosal macrophages leading to the transcriptional upregulation of pro-IL-1β, mediated by receptors of the innate immune system. A second step leads to the activation of the NLRP3 inflammasome followed by secretion of active IL-1β, which is a key cytokine for the initiation and progression of inflammatory processes. Thus, the NLRP3 inflammasome could serve as a novel target for drug development for IBD.

1.6 Abkürzungsverzeichnis

ACAT	A:Cholesterin-Acyltransferase
ApoE	Apolipoprotein E
ASC	apoptosis-associated speck-like protein containing a CARD
ATP	Adenosintriphosphat
BIR	baculovirus inhibitor of apoptosis protein repeats
CAPS	cryopyrin-associated periodic syndrome
CARD	caspase recruitment domain
CINCA	chronic infantile cutaneous neurological articular syndrome
CRD	C-terminal repressor domain
DAMP	danger-associated molecular pattern
DNA	deoxyribonucleic acid
DSS	dextransulfate sodium
EMCV	Enzephalomyokarditis-Virus
FCAS	familial cold autoinflammatory syndrome
HMGB1	high mobility group protein B1
ICE	interleukin-1 converting enzyme
IFN	Interferon
IL	Interleukin
IL-1RA	Interleukin-1-Rezeptor-Antagonist
IPAF	ICE protease activating factor
IPS-1	IFN-β promoter stimulator 1
IRF	interferon regulatory factor
LDL	low density lipoprotein
LGP-2	laboratory of genetics and physiology 2
LPS	Lipopolysaccharid
LRR	leucine rich repeats
MAMP	microorganism-associated molecular pattern
MAPK	mitogen-activated protein kinase
MAVS	mitochondrial antiviral signaling protein
MDA-5	melanoma differentiation-associated gene 5
MDP	muramyl dipeptide
MWS	Muckle-Wells syndrome
MyD88	myeloid differentiation primary response gene (88)
NF-κB	nuclear factor 'κ-light-chain-enhancer' of activated B-cells
NLR	NOD-like receptor
NOD	nucleotide oligomerization domain
PAMP	pathogen-associated molecular pattern
poly(I:C)	polyinosinic:polycytidylic acid
PRR	pattern recognition receptor
RIG-I	retinoic acid-inducible gene 1
RLR	RIG-I-like receptors
RNA	ribonucleic acid
ROS	reactive oxygen species
TIR	Toll-IL-1 receptor homologous domain
TLR	Toll-like receptor
TNF-α	tumor necrosis factor α
TRADD	TNF receptor type 1-associated DEATH domain
TRIF	TIR domain containing adapter inducing interferon-β
VISA	virus-induced signaling adapter

1.6 Literatur

1. Basset C, Holton J, O'Mahony R, Roitt I. 2003. Innate immunity and pathogen-host interaction. *Vaccine* 21 Suppl 2: S12-23
2. Chaplin DD. Overview of the immune response. *J Allergy Clin Immunol* 125: S3-23
3. Danilova N. 2006. The evolution of immune mechanisms. *J Exp Zool B Mol Dev Evol* 306: 496-520
4. Janeway CA, Jr., Medzhitov R. 2002. Innate immune recognition. *Annu Rev Immunol* 20: 197-216
5. Matzinger P. 2002. The danger model: a renewed sense of self. *Science* 296: 301-5
6. Medzhitov R, Janeway CA, Jr. 1997. Innate immunity: the virtues of a nonclonal system of recognition. *Cell* 91: 295-8
7. Takeda K, Akira S. 2005. Toll-like receptors in innate immunity. *Int Immunol* 17: 1-14
8. Yoneyama M, Fujita T. 2007. RIG-I family RNA helicases: cytoplasmic sensor for antiviral innate immunity. *Cytokine Growth Factor Rev* 18: 545-51
9. Anderson KV, Bokla L, Nusslein-Volhard C. 1985. Establishment of dorsal-ventral polarity in the Drosophila embryo: the induction of polarity by the Toll gene product. *Cell* 42: 791-8
10. Lemaitre B, Nicolas E, Michaut L, Reichhart JM, Hoffmann JA. 1996. The dorsoventral regulatory gene cassette spatzle/Toll/cactus controls the potent antifungal response in Drosophila adults. *Cell* 86: 973-83
11. Akira S, Uematsu S, Takeuchi O. 2006. Pathogen recognition and innate immunity. *Cell* 124: 783-801
12. Medzhitov R. 2007. Recognition of microorganisms and activation of the immune response. *Nature* 449: 819-26
13. Beutler BA. 2009. TLRs and innate immunity. *Blood* 113: 1399-407
14. Yoneyama M, Fujita T. 2008. Structural mechanism of RNA recognition by the RIG-I-like receptors. *Immunity* 29: 178-81
15. Kato H, Sato S, Yoneyama M, Yamamoto M, Uematsu S, Matsui K, Tsujimura T, Takeda K, Fujita T, Takeuchi O, Akira S. 2005. Cell type-specific involvement of RIG-I in antiviral response. *Immunity* 23: 19-28
16. Kato H, Takeuchi O, Sato S, Yoneyama M, Yamamoto M, Matsui K, Uematsu S, Jung A, Kawai T, Ishii KJ, Yamaguchi O, Otsu K, Tsujimura T, Koh CS, Reis e Sousa C, Matsuura Y, Fujita T, Akira S. 2006. Differential roles of MDA5 and RIG-I helicases in the recognition of RNA viruses. *Nature* 441: 101-5
17. Hornung V, Ellegast J, Kim S, Brzozka K, Jung A, Kato H, Poeck H, Akira S, Conzelmann KK, Schlee M, Endres S, Hartmann G. 2006. 5'-Triphosphate RNA is the ligand for RIG-I. *Science* 314: 994-7
18. Saito T, Owen DM, Jiang F, Marcotrigiano J, Gale M, Jr. 2008. Innate immunity induced by composition-dependent RIG-I recognition of hepatitis C virus RNA. *Nature* 454: 523-7
19. Takeuchi O, Akira S. 2008. MDA5/RIG-I and virus recognition. *Curr Opin Immunol* 20: 17-22
20. Gitlin L, Barchet W, Gilfillan S, Cella M, Beutler B, Flavell RA, Diamond MS, Colonna M. 2006. Essential role of mda-5 in type I IFN responses to polyriboinosinic:polyribocytidylic acid and encephalomyocarditis picornavirus. *Proc Natl Acad Sci U S A* 103: 8459-64
21. Franchi L, Park JH, Shaw MH, Marina-Garcia N, Chen G, Kim YG, Nunez G. 2008. Intracellular NOD-like receptors in innate immunity, infection and disease. *Cell Microbiol* 10: 1-8

22. Martinon F. 2008. Detection of immune danger signals by NALP3. *J Leukoc Biol* 83: 507-11
23. Kawai T, Akira S. 2009. The roles of TLRs, RLRs and NLRs in pathogen recognition. *Int Immunol* 21: 317-37
24. Ting JP, Willingham SB, Bergstralh DT. 2008. NLRs at the intersection of cell death and immunity. *Nat Rev Immunol* 8: 372-9
25. Inohara N, Nunez G. 2003. NODs: intracellular proteins involved in inflammation and apoptosis. *Nat Rev Immunol* 3: 371-82
26. Inohara, Chamaillard, McDonald C, Nunez G. 2005. NOD-LRR proteins: role in host-microbial interactions and inflammatory disease. *Annu Rev Biochem* 74: 355-83
27. Franchi L, Warner N, Viani K, Nunez G. 2009. Function of Nod-like receptors in microbial recognition and host defense. *Immunol Rev* 227: 106-28
28. Martinon F, Burns K, Tschopp J. 2002. The inflammasome: a molecular platform triggering activation of inflammatory caspases and processing of proIL-beta. *Mol Cell* 10: 417-26
29. Latz E. The inflammasomes: mechanisms of activation and function. *Curr Opin Immunol* 22: 28-33
30. Boyden ED, Dietrich WF. 2006. Nalp1b controls mouse macrophage susceptibility to anthrax lethal toxin. *Nat Genet* 38: 240-4
31. Faustin B, Lartigue L, Bruey JM, Luciano F, Sergienko E, Bailly-Maitre B, Volkmann N, Hanein D, Rouiller I, Reed JC. 2007. Reconstituted NALP1 inflammasome reveals two-step mechanism of caspase-1 activation. *Mol Cell* 25: 713-24
32. Franchi L, Eigenbrod T, Munoz-Planillo R, Nunez G. 2009. The inflammasome: a caspase-1-activation platform that regulates immune responses and disease pathogenesis. *Nat Immunol* 10: 241-7
33. Gross O, Poeck H, Bscheider M, Dostert C, Hannesschlager N, Endres S, Hartmann G, Tardivel A, Schweighoffer E, Tybulewicz V, Mocsai A, Tschopp J, Ruland J. 2009. Syk kinase signalling couples to the Nlrp3 inflammasome for anti-fungal host defence. *Nature* 459: 433-6
34. Mariathasan S, Weiss DS, Newton K, McBride J, O'Rourke K, Roose-Girma M, Lee WP, Weinrauch Y, Monack DM, Dixit VM. 2006. Cryopyrin activates the inflammasome in response to toxins and ATP. *Nature* 440: 228-32
35. Kanneganti TD, Ozoren N, Body-Malapel M, Amer A, Park JH, Franchi L, Whitfield J, Barchet W, Colonna M, Vandenabeele P, Bertin J, Coyle A, Grant EP, Akira S, Nunez G. 2006. Bacterial RNA and small antiviral compounds activate caspase-1 through cryopyrin/Nalp3. *Nature* 440: 233-6
36. Muruve DA, Petrilli V, Zaiss AK, White LR, Clark SA, Ross PJ, Parks RJ, Tschopp J. 2008. The inflammasome recognizes cytosolic microbial and host DNA and triggers an innate immune response. *Nature* 452: 103-7
37. Yamasaki K, Muto J, Taylor KR, Cogen AL, Audish D, Bertin J, Grant EP, Coyle AJ, Misaghi A, Hoffman HM, Gallo RL. 2009. NLRP3/cryopyrin is necessary for interleukin-1beta (IL-1beta) release in response to hyaluronan, an endogenous trigger of inflammation in response to injury. *J Biol Chem* 284: 12762-71
38. Halle A, Hornung V, Petzold GC, Stewart CR, Monks BG, Reinheckel T, Fitzgerald KA, Latz E, Moore KJ, Golenbock DT. 2008. The NALP3 inflammasome is involved in the innate immune response to amyloid-beta. *Nat Immunol* 9: 857-65
39. Martinon F, Petrilli V, Mayor A, Tardivel A, Tschopp J. 2006. Gout-associated uric acid crystals activate the NALP3 inflammasome. *Nature* 440: 237-41
40. Duewell P, Kono H, Rayner KJ, Sirois CM, Vladimer G, Bauernfeind FG, Abela GS, Franchi L, Nunez G, Schnurr M, Espevik T, Lien E, Fitzgerald KA, Rock KL, Moore KJ, Wright SD, Hornung V, Latz E. 2010. NLRP3

inflammasomes are required for atherogenesis and activated by cholesterol crystals. *Nature* 464: 1357-61
41. Hornung V, Bauernfeind F, Halle A, Samstad EO, Kono H, Rock KL, Fitzgerald KA, Latz E. 2008. Silica crystals and aluminum salts activate the NALP3 inflammasome through phagosomal destabilization. *Nat Immunol* 9: 847-56
42. Cassel SL, Eisenbarth SC, Iyer SS, Sadler JJ, Colegio OR, Tephly LA, Carter AB, Rothman PB, Flavell RA, Sutterwala FS. 2008. The Nalp3 inflammasome is essential for the development of silicosis. *Proc Natl Acad Sci U S A* 105: 9035-40
43. Dostert C, Petrilli V, Van Bruggen R, Steele C, Mossman BT, Tschopp J. 2008. Innate immune activation through Nalp3 inflammasome sensing of asbestos and silica. *Science* 320: 674-7
44. Feldmeyer L, Keller M, Niklaus G, Hohl D, Werner S, Beer HD. 2007. The inflammasome mediates UVB-induced activation and secretion of interleukin-1beta by keratinocytes. *Curr Biol* 17: 1140-5
45. Allen IC, Scull MA, Moore CB, Holl EK, McElvania-TeKippe E, Taxman DJ, Guthrie EH, Pickles RJ, Ting JP. 2009. The NLRP3 inflammasome mediates in vivo innate immunity to influenza A virus through recognition of viral RNA. *Immunity* 30: 556-65
46. Poeck H, Bscheider M, Gross O, Finger K, Roth S, Rebsamen M, Hannesschlager N, Schlee M, Rothenfusser S, Barchet W, Kato H, Akira S, Inoue S, Endres S, Peschel C, Hartmann G, Hornung V, Ruland J. Recognition of RNA virus by RIG-I results in activation of CARD9 and inflammasome signaling for interleukin 1 beta production. *Nat Immunol* 11: 63-9
47. Duncan JA, Gao X, Huang MT, O'Connor BP, Thomas CE, Willingham SB, Bergstralh DT, Jarvis GA, Sparling PF, Ting JP. 2009. Neisseria gonorrhoeae activates the proteinase cathepsin B to mediate the signaling activities of the NLRP3 and ASC-containing inflammasome. *J Immunol* 182: 6460-9
48. Craven RR, Gao X, Allen IC, Gris D, Bubeck Wardenburg J, McElvania-Tekippe E, Ting JP, Duncan JA. 2009. Staphylococcus aureus alpha-hemolysin activates the NLRP3-inflammasome in human and mouse monocytic cells. *PLoS One* 4: e7446
49. Gurcel L, Abrami L, Girardin S, Tschopp J, van der Goot FG. 2006. Caspase-1 activation of lipid metabolic pathways in response to bacterial pore-forming toxins promotes cell survival. *Cell* 126: 1135-45
50. Eisenbarth SC. 2008. Use and limitations of alum-based models of allergy. *Clin Exp Allergy* 38: 1572-5
51. Franchi L, Nunez G. 2008. The Nlrp3 inflammasome is critical for aluminium hydroxide-mediated IL-1beta secretion but dispensable for adjuvant activity. *Eur J Immunol* 38: 2085-9
52. Kool M, Petrilli V, De Smedt T, Rolaz A, Hammad H, van Nimwegen M, Bergen IM, Castillo R, Lambrecht BN, Tschopp J. 2008. Cutting edge: alum adjuvant stimulates inflammatory dendritic cells through activation of the NALP3 inflammasome. *J Immunol* 181: 3755-9
53. Li H, Willingham SB, Ting JP, Re F. 2008. Cutting edge: inflammasome activation by alum and alum's adjuvant effect are mediated by NLRP3. *J Immunol* 181: 17-21
54. Zhou R, Tardivel A, Thorens B, Choi I, Tschopp J. Thioredoxin-interacting protein links oxidative stress to inflammasome activation. *Nat Immunol* 11: 136-40
55. Schroder K, Tschopp J. The inflammasomes. *Cell* 140: 821-32
56. Kanneganti TD, Lamkanfi M, Kim YG, Chen G, Park JH, Franchi L, Vandenabeele P, Nunez G. 2007. Pannexin-1-mediated recognition of

bacterial molecules activates the cryopyrin inflammasome independent of Toll-like receptor signaling. *Immunity* 26: 433-43
57. Cruz CM, Rinna A, Forman HJ, Ventura AL, Persechini PM, Ojcius DM. 2007. ATP activates a reactive oxygen species-dependent oxidative stress response and secretion of proinflammatory cytokines in macrophages. *J Biol Chem* 282: 2871-9
58. Bauernfeind FG, Horvath G, Stutz A, Alnemri ES, MacDonald K, Speert D, Fernandes-Alnemri T, Wu J, Monks BG, Fitzgerald KA, Hornung V, Latz E. 2009. Cutting edge: NF-kappaB activating pattern recognition and cytokine receptors license NLRP3 inflammasome activation by regulating NLRP3 expression. *J Immunol* 183: 787-91
59. Stutz A, Golenbock DT, Latz E. 2009. Inflammasomes: too big to miss. *J Clin Invest* 119: 3502-11
60. Dinarello CA. 2009. Interleukin-1beta and the autoinflammatory diseases. *N Engl J Med* 360: 2467-70
61. Brydges SD, Mueller JL, McGeough MD, Pena CA, Misaghi A, Gandhi C, Putnam CD, Boyle DL, Firestein GS, Horner AA, Soroosh P, Watford WT, O'Shea JJ, Kastner DL, Hoffman HM. 2009. Inflammasome-mediated disease animal models reveal roles for innate but not adaptive immunity. *Immunity* 30: 875-87
62. Meng G, Zhang F, Fuss I, Kitani A, Strober W. 2009. A mutation in the Nlrp3 gene causing inflammasome hyperactivation potentiates Th17 cell-dominant immune responses. *Immunity* 30: 860-74
63. McGonagle D, Tan AL, Madden J, Emery P, McDermott MF. 2008. Successful treatment of resistant pseudogout with anakinra. *Arthritis Rheum* 58: 631-3
64. McGonagle D, Tan AL, Shankaranarayana S, Madden J, Emery P, McDermott MF. 2007. Management of treatment resistant inflammation of acute on chronic tophaceous gout with anakinra. *Ann Rheum Dis* 66: 1683-4
65. So A, De Smedt T, Revaz S, Tschopp J. 2007. A pilot study of IL-1 inhibition by anakinra in acute gout. *Arthritis Res Ther* 9: R28
66. Terkeltaub R, Sundy JS, Schumacher HR, Murphy F, Bookbinder S, Biedermann S, Wu R, Mellis S, Radin A. 2009. The interleukin 1 inhibitor rilonacept in treatment of chronic gouty arthritis: results of a placebo-controlled, monosequence crossover, non-randomised, single-blind pilot study. *Ann Rheum Dis* 68: 1613-7
67. Mossman BT, Churg A. 1998. Mechanisms in the pathogenesis of asbestosis and silicosis. *Am J Respir Crit Care Med* 157: 1666-80
68. Rimal B, Greenberg AK, Rom WN. 2005. Basic pathogenetic mechanisms in silicosis: current understanding. *Curr Opin Pulm Med* 11: 169-73
69. Doz E, Noulin N, Boichot E, Guenon I, Fick L, Le Bert M, Lagente V, Ryffel B, Schnyder B, Quesniaux VF, Couillin I. 2008. Cigarette smoke-induced pulmonary inflammation is TLR4/MyD88 and IL-1R1/MyD88 signaling dependent. *J Immunol* 180: 1169-78
70. Weiner HL, Frenkel D. 2006. Immunology and immunotherapy of Alzheimer's disease. *Nat Rev Immunol* 6: 404-16
71. Meyer-Luehmann M, Spires-Jones TL, Prada C, Garcia-Alloza M, de Calignon A, Rozkalne A, Koenigsknecht-Talboo J, Holtzman DM, Bacskai BJ, Hyman BT. 2008. Rapid appearance and local toxicity of amyloid-beta plaques in a mouse model of Alzheimer's disease. *Nature* 451: 720-4
72. Simard AR, Soulet D, Gowing G, Julien JP, Rivest S. 2006. Bone marrow-derived microglia play a critical role in restricting senile plaque formation in Alzheimer's disease. *Neuron* 49: 489-502

73. Itagaki S, McGeer PL, Akiyama H, Zhu S, Selkoe D. 1989. Relationship of microglia and astrocytes to amyloid deposits of Alzheimer disease. *J Neuroimmunol* 24: 173-82
74. Griffin WS, Stanley LC, Ling C, White L, MacLeod V, Perrot LJ, White CL, 3rd, Araoz C. 1989. Brain interleukin 1 and S-100 immunoreactivity are elevated in Down syndrome and Alzheimer disease. *Proc Natl Acad Sci U S A* 86: 7611-5
75. Watanabe H, Gaide O, Petrilli V, Martinon F, Contassot E, Roques S, Kummer JA, Tschopp J, French LE. 2007. Activation of the IL-1beta-processing inflammasome is involved in contact hypersensitivity. *J Invest Dermatol* 127: 1956-63
76. Spranger J, Kroke A, Mohlig M, Hoffmann K, Bergmann MM, Ristow M, Boeing H, Pfeiffer AF. 2003. Inflammatory cytokines and the risk to develop type 2 diabetes: results of the prospective population-based European Prospective Investigation into Cancer and Nutrition (EPIC)-Potsdam Study. *Diabetes* 52: 812-7
77. Maedler K, Dharmadhikari G, Schumann DM, Storling J. 2009. Interleukin-1 beta targeted therapy for type 2 diabetes. *Expert Opin Biol Ther* 9: 1177-88
78. Schroder K, Zhou R, Tschopp J. The NLRP3 inflammasome: a sensor for metabolic danger? *Science* 327: 296-300
79. Villani AC, Lemire M, Fortin G, Louis E, Silverberg MS, Collette C, Baba N, Libioulle C, Belaiche J, Bitton A, Gaudet D, Cohen A, Langelier D, Fortin PR, Wither JE, Sarfati M, Rutgeerts P, Rioux JD, Vermeire S, Hudson TJ, Franchimont D. 2009. Common variants in the NLRP3 region contribute to Crohn's disease susceptibility. *Nat Genet* 41: 71-6
80. Loher F, Bauer C, Landauer N, Schmall K, Siegmund B, Lehr HA, Dauer M, Schoenharting M, Endres S, Eigler A. 2004. The interleukin-1 beta-converting enzyme inhibitor pralnacasan reduces dextran sulfate sodium-induced murine colitis and T helper 1 T-cell activation. *J Pharmacol Exp Ther* 308: 583-90

2. Ergebnisse (publizierte Originalarbeiten)

2.1 Originalarbeit: Duewell P., Kono H., et al. *Nature* 2010

NLRP3 inflammasomes are required for atherogenesis and activated by cholesterol crystals early in disease

Peter Duewell, Hajime Kono, Katey J. Rayner, Cherilyn M. Sirois, Gregory Vladimer, Franz G. Bauernfeind, George S. Abela, Luigi Franchi, Gabriel Nuñez, Max Schnurr, Terje Espevik, Egil Lien, Katherine A. Fitzgerald, Kenneth L. Rock, Kathryn J. Moore, Samuel D Wright, Veit Hornung and Eicke Latz

Nature. 2010 Apr 29;464(7293):1357-61

LETTERS

NLRP3 inflammasomes are required for atherogenesis and activated by cholesterol crystals

Peter Duewell[1,3]*, Hajime Kono[2]*, Katey J. Rayner[4,5], Cherilyn M. Sirois[1], Gregory Vladimer[1], Franz G. Bauernfeind[6], George S. Abela[8], Luigi Franchi[9], Gabriel Nuñez[9], Max Schnurr[3], Terje Espevik[10], Egil Lien[1], Katherine A. Fitzgerald[1], Kenneth L. Rock[2], Kathryn J. Moore[4,5], Samuel D. Wright[11], Veit Hornung[5]* & Eicke Latz[1,7,10]*

The inflammatory nature of atherosclerosis is well established but the agent(s) that incite inflammation in the artery wall remain largely unknown. Germ-free animals are susceptible to atherosclerosis, suggesting that endogenous substances initiate the inflammation[1]. Mature atherosclerotic lesions contain macroscopic deposits of cholesterol crystals in the necrotic core, but their appearance late in atherogenesis had been thought to disqualify them as primary inflammatory stimuli. However, using a new microscopic technique, we revealed that minute cholesterol crystals are present in early diet-induced atherosclerotic lesions and that their appearance in mice coincides with the first appearance of inflammatory cells. Other crystalline substances can induce inflammation by stimulating the caspase-1-activating NLRP3 (NALP3 or cryopyrin) inflammasome[2,3], which results in cleavage and secretion of interleukin (IL)-1 family cytokines. Here we show that cholesterol crystals activate the NLRP3 inflammasome in phagocytes *in vitro* in a process that involves phagolysosomal damage. Similarly, when injected intraperitoneally, cholesterol crystals induce acute inflammation, which is impaired in mice deficient in components of the NLRP3 inflammasome, cathepsin B, cathepsin L or IL-1 molecules. Moreover, when mice deficient in low-density lipoprotein receptor (LDLR) were bone-marrow transplanted with NLRP3-deficient, ASC (also known as PYCARD)-deficient or IL-1α/β-deficient bone marrow and fed on a high-cholesterol diet, they had markedly decreased early atherosclerosis and inflammasome-dependent IL-18 levels. Minimally modified LDL can lead to cholesterol crystallization concomitant with NLRP3 inflammasome priming and activation in macrophages. Although there is the possibility that oxidized LDL activates the NLRP3 inflammasome *in vivo*, our results demonstrate that crystalline cholesterol acts as an endogenous danger signal and its deposition in arteries or elsewhere is an early cause rather than a late consequence of inflammation. These findings provide new insights into the pathogenesis of atherosclerosis and indicate new potential molecular targets for the therapy of this disease.

Cholesterol, an indispensable lipid in vertebrates, is effectively insoluble in aqueous environments, and elaborate molecular mechanisms have evolved that regulate cholesterol synthesis and its transport in fluids[4]. Cholesterol crystals are recognized as a hallmark of atherosclerotic lesions[5] and their appearance assists the histopathological classification of advanced atherosclerotic lesions[6]. However, crystalline cholesterol is soluble in the organic solvents used in histology, so that the presence of large crystals is identifiable but only indirectly as so-called cholesterol crystal clefts, which delineate the space that was occupied before sample preparation[7]. The large cholesterol crystal clefts in atherosclerotic plaques were typically observed only in advanced lesions; crystal deposition was therefore thought to arise late in this disease. However, given that atherosclerosis is intimately linked to cholesterol levels, we were interested to determine when and where cholesterol crystals first appear during atherogenesis.

We fed atherosclerosis-prone Apo-E-deficient mice on a high cholesterol diet to induce atherosclerosis[8,9] and used a combination of laser reflection and fluorescence confocal microscopy[3] to identify crystalline materials and immune cells. Many small crystals appeared as early as two weeks after the start of the atherogenic diet within small accumulations of subendothelial immune cells in very early atherosclerotic sinus lesions (Fig. 1a, b and Supplementary Figs 1 and 2). The reflective material was identified by filipin staining as being mostly cholesterol crystals (not shown). Crystal deposition and immune-cell recruitment increased steadily with diet feeding, and the appearance of crystals was correlated with that of macrophages ($r^2 = 0.99$, $P < 0.001$) (Fig. 1a–e). Cholesterol crystals were detected not only in necrotic cores but also in subendothelial areas and found to localize both inside and outside cells (Fig. 1b). In corresponding haematoxylin/eosin-stained sections cholesterol crystal clefts were visible only after 8 weeks of diet, and smaller crystals remained invisible (Fig. 1a). As expected, we failed to detect macrophages or accumulation of crystals in the aortic sinus sections in mice fed on a regular chow diet (Fig. 1a, b, bottom panels). In addition, in human atherosclerotic lesions small crystals were abundant in areas rich in immune cells (Supplementary Figs 3 and 4). These studies establish that crystals emerge at the earliest time points of diet-induced atherogenesis together with the appearance of immune cells in the subendothelial space.

Various crystals that are linked to tissue inflammation, as well as pore-forming toxins or extracellular ATP, can activate IL-1 family cytokines through the triggering of NLRP3 (ref. 10). Of note, cellular priming through nuclear factor (NF)-κB activation leads to the induction of pro-forms of the IL-1 family cytokines and NLRP3 itself, a step that is required for NLRP3 activation, at least *in vitro*[11]. To test whether cholesterol crystals could activate the release of IL-1β, we incubated lipopolysaccharide (LPS)-primed human peripheral blood mononuclear cells (PBMCs) with cholesterol crystals. Cholesterol crystals induced a robust, dose-responsive release of cleaved IL-1β

[1]Department of Infectious Diseases and Immunology and [2]Department of Pathology, University of Massachusetts Medical School, Worcester, Massachusetts 01605, USA. [3]Department of Medicine, Division of Gastroenterology, University of Munich, 80336 Munich, Germany. [4]Leon H. Charney Division of Cardiology, New York University, New York, New York 10016, USA. [5]Harvard Medical School, Lipid Metabolism Unit, Massachusetts General Hospital, Boston, Massachusetts 02114, USA. [6]Institute of Clinical Chemistry and Pharmacology and [7]Institute of Innate Immunology, University Hospitals, University of Bonn, 53127 Bonn, Germany. [8]Department of Medicine, Division of Cardiology, Michigan State University, East Lansing, Michigan 48824, USA. [9]Department of Pathology, University of Michigan Medical School, Ann Arbor, Michigan 48109, USA. [10]Institute of Cancer Research and Molecular Medicine, Norwegian University of Science and Technology, Trondheim, 7491, Norway. [11]Cardiovascular Therapeutics, CSL Limited, Parkville, Victoria 3052, Australia. *These authors contributed equally to this work.

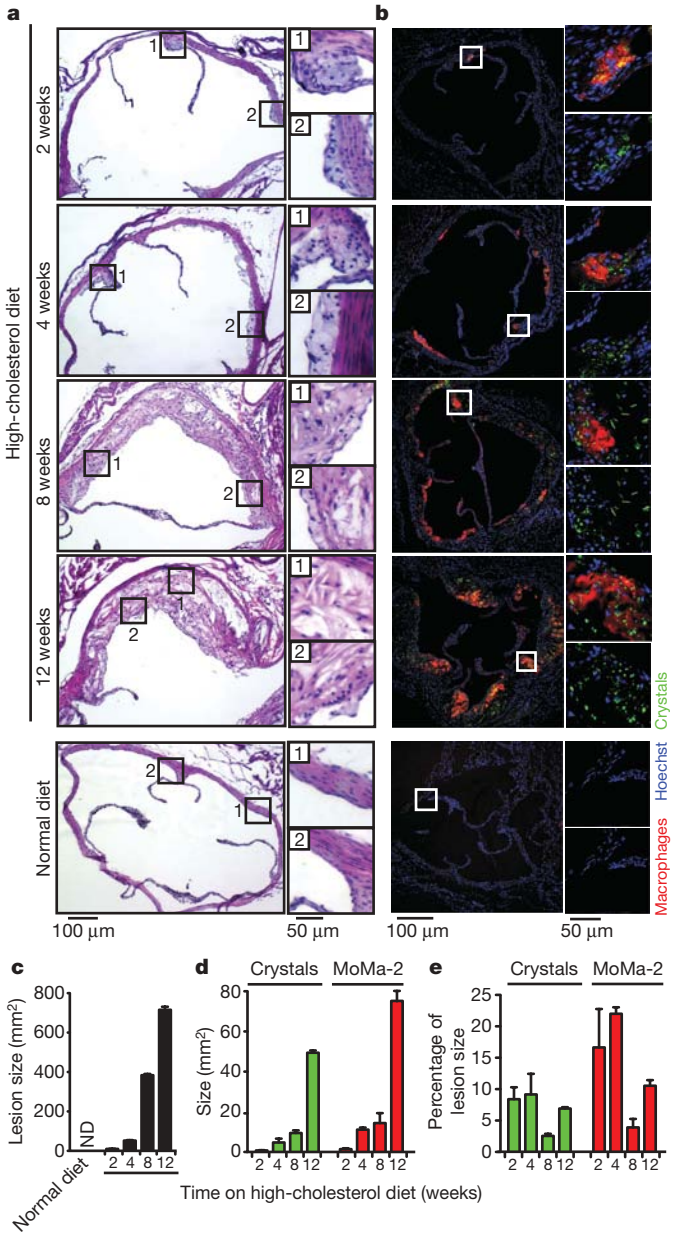

Figure 1 | Cholesterol crystals appear in early atherosclerotic lesions. **a**, **b**, Haematoxylin/eosin staining (**a**) and confocal fluorescence and reflection microscopy (**b**) of adjacent aortic sinus sections of Apo-E knockout mice fed on a high-cholesterol diet as indicated or on a normal diet (bottom panels). Areas in white or black boxes are shown enlarged; the crystal reflection signal is colour-coded green. **c**–**e**, Quantification of lesion size (**c**), amount of crystal or macrophage marker MoMa-2 staining presented as absolute values (**d**) or as a percentage of lesion size (**e**). ND, not detected. In **a** and **b** sections representative of three mice from each group are shown. Means and s.e.m. are shown in **c**, **d** and **e**.

in a caspase-1-dependent manner (Fig. 2a, b). Cholesterol crystals added to unprimed cells did not release IL-1β into the supernatant, indicating the absence of any contaminants that would be sufficient for the priming of cells (Fig. 2a)[11]. IL-1 cytokines are processed by caspase-1, which can be activated by various inflammasomes[9]. Indeed, as previously observed with other crystals, cholesterol crystals induced caspase-1 cleavage and IL-1β release in wild-type but not in NLRP3-deficient or ASC-deficient macrophages (Fig. 2c, d). Transfected double-stranded DNA (poly(dA-dT)•poly(dT-dA)), a control activator that induces the AIM-2 inflammasome[12], activated caspase-1 and induced IL-1β release in an ASC-dependent but NLRP3-independent manner, as expected (Fig. 2c, d). In addition, mouse macrophages also produced cleaved IL-18, another IL-1 family member that is processed by inflammasomes (Supplementary Fig. 5a). We also found that chemically pure synthetic cholesterol crystals activated NLRP3, providing further evidence that cholesterol crystals themselves rather than contaminating molecules were the biologically active material (Supplementary Fig. 5b). Priming of cells for NLRP3 activation could be achieved by other pro-inflammatory substances such as cell wall components of Gram-positive bacteria (Supplementary Fig. 5c). Moreover, minimally modified low-density lipoprotein (LDL) also primed cells for NLRP3 activation (Supplementary Fig. 5d)[13]. Taken together, these data establish that crystalline cholesterol leads to NLRP3 inflammasome activation in human and mouse immune cells.

For further elucidation of the mechanisms involved in cholesterol crystal recognition, we inhibited phagocytosis pharmacologically with cytochalasin D or lantriculin A. We found that these agents inhibited NLRP3 activation by crystals but not by the AIM2 activator poly(dA-dT)•poly(dT-dA) (Fig. 3a and Supplementary Fig. 6a, c, d). To follow the fate of the internalized particles, we analysed macrophages incubated with cholesterol crystals by combined confocal reflection and fluorescence microscopy. Cholesterol crystals induced profound swelling in a fraction of cells (Fig. 3b), as observed for other aggregated materials[3,14]. Phagolysosomal membranes contain lipid raft components[15], which allowed us to stain the surface of cells with the raft marker choleratoxin B labelled with one fluorescent colour and also to label internal phagolysosomal membranes after cell permeabilization with differently fluorescing choleratoxin B. Indeed, in macrophages that had previously ingested cholesterol crystals, this staining revealed that some cholesterol crystals lacked phagolysosomal membranes and resided in the cytosol of a fraction of cells, thus indirectly indicating crystal-induced phagolysosomal membrane rupture (Fig. 3c). This finding was further supported by crystal-induced translocation of soluble lysosomal markers into the cytosol (see below). In addition, cholesterol crystals dose-responsively led to a loss of lysosomal acridine orange fluorescence, further confirming lysosomal disruption (Supplementary Fig. 6e). These studies suggest that cholesterol-crystal-induced lysosomal damage in macrophages leads to the translocation of phagolysosomal content into the cytosol. In further experiments we found that the inhibition of lysosomal acidification or cathepsin activity blocked the ability of cholesterol crystals to induce IL-1β secretion (Supplementary Fig. 6f). Similarly, analysis of cells from mice deficient in single cathepsins (B or L) also showed that cholesterol crystals led to a diminished release of IL-1β in comparison with wild-type cells. However, the dependence of cholesterol-crystal-induced IL-1β release on single cathepsins was less pronounced at higher doses, suggesting functional redundancy of cathepsin B and L or potentially additional proteases (Fig. 3d). Taken together, these experiments suggest that cholesterol crystals induce translocation of the lysosomal proteolytic contents, which can be sensed by the NLRP3 inflammasome by as yet undefined mechanisms.

It has previously been demonstrated that oxidized LDL, a major lipid species deposited in vessels, has the potential to damage lysosomal membranes[16]. We found that macrophages incubated with oxidized LDL internalized this material and nucleated crystals in large, swollen, phagolysosomal compartments (Fig. 3e); in some cells these compartments ruptured with translocation of the fluorescent marker dye into the cytosol (Fig. 3e, arrows). A time-course analysis revealed that small crystals appeared as early as 1 h after incubation with oxidized LDL (not shown), and larger crystals were visible after longer incubation times (Fig. 3f). It is likely that cholesterol crystals form as a result of the activity of acid cholesterol ester hydolases, which transform cholesteryl esters supplied by oxidized LDL into free cholesterol. As indicated above, minimally modified LDL can prime cells for the NLRP3 inflammasome activation (Supplementary Fig. 5d). Recent evidence suggests that this priming proceeds through the activation of a TLR4/6 homodimer and CD36 (ref. 13). This, together with the propensity of minimally modified LDL to form

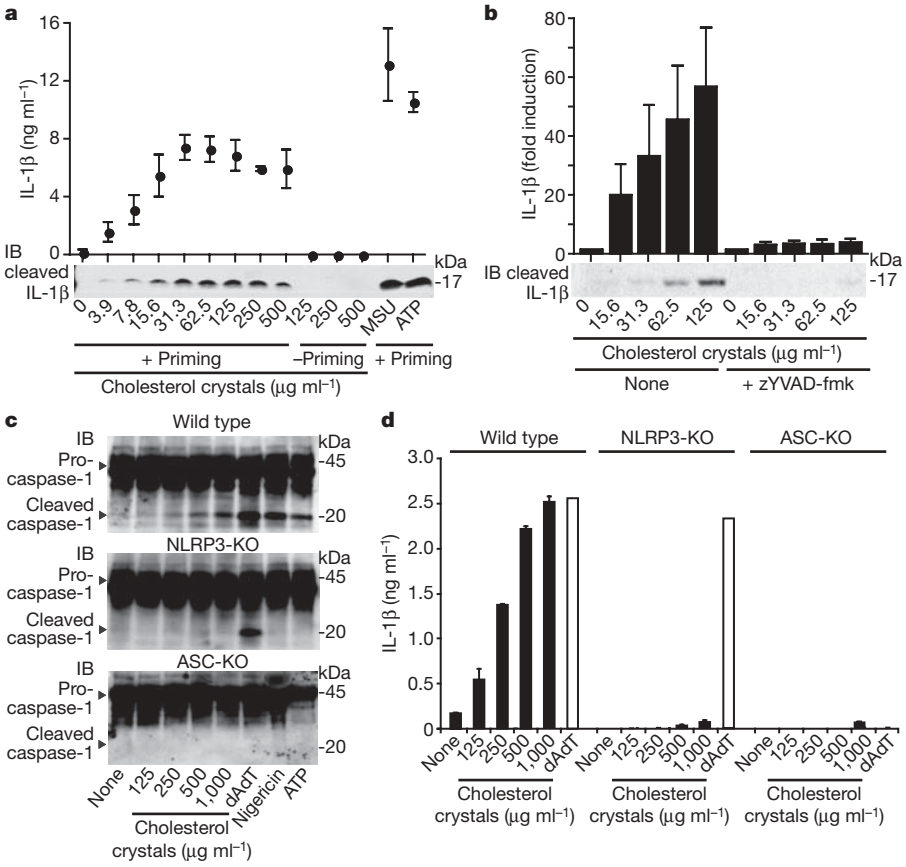

Figure 2 | Cholesterol crystals activate the NLRP3 inflammasome. **a**, **b**, Resting or LPS-primed human PBMCs were treated with cholesterol crystals as indicated, monosodium urate (MSU) crystals (250 μg ml^{-1}) or ATP in the absence (**a**) or presence (**b**) of the caspase-1 inhibitor zYVAD-fmk (10 μM). ELISA and immunoblotting (IB) were performed for IL-1β. **c**, **d**, IB for caspase-1 in supernatants and cell lysates (**c**) or ELISA for IL-1β in supernatants (**d**) from LPS-primed wild-type, NLRP3-deficient (KO) or ASC-deficient macrophages stimulated with cholesterol crystals, transfected double-stranded DNA (poly(dA-dT)•poly(dT-dA)), nigericin or ATP. Means and s.e.m. for four donors are shown in **a** and **b**; one out of three independent experiments is shown in each of **c** and **d**.

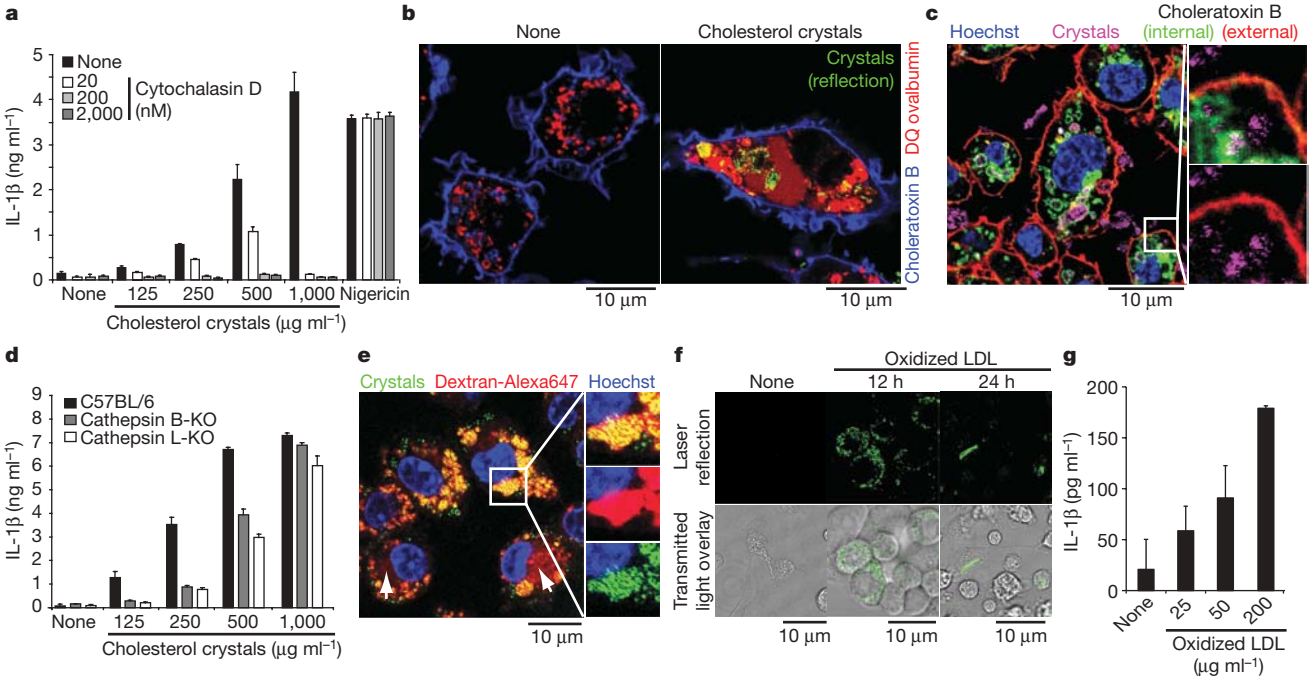

Figure 3 | Cholesterol crystals activate the NLRP3 inflammasome by inducing lysosomal damage. **a**, IL-1β ELISA of supernatants from LPS-primed mouse macrophages stimulated with cholesterol crystals or nigericin in the presence or absence of cytochalasin D. **b**, **c**, Combined confocal fluorescence and reflection microscopy of mouse macrophages incubated with DQ ovalbumin alone (**b**, left) or together with cholesterol crystals (125 μg ml^{-1}) (**b**, right; **c**) for 2 h; plasma membrane was stained with Alexa647-conjugated choleratoxin B (**b**, **c**). **c**, Cells were fixed and permeabilized (0.05% saponin) and internal membranes were additionally stained with Alexa555-conjugated choleratoxin B. Nuclei were stained with Hoechst dye. **d**, IL-1β ELISA of supernatants from LPS-primed mouse macrophages stimulated with cholesterol crystals. **e**, **f**, Mouse macrophages stimulated with oxidized LDL for the indicated durations and fluorescent dextran (**e**, 20 h) were imaged by combined confocal fluorescence and reflection microscopy. **g**, Unprimed mouse macrophages were incubated for 24 h with oxidized LDL as indicated, and IL-1β in supernatants was measured by ELISA. In each of **a**, **d** and **g**, one of three independent experiments is shown (means and s.d.). Representative images of five (**b**, **c**) and two (**e**, **f**) independent experiments are shown.

crystals and to rupture lysosomal membranes, suggests that these LDL species could be sufficient to provide both signals 1 and 2 needed to activate IL-1β release from cells. Indeed, after 24 h of incubation we observed a spontaneous release of IL-1β in the absence of further stimulation of NLRP3 inflammasomes (Fig. 3g).

In mouse atherosclerotic lesions we identified not only macrophages and dendritic cells but also neutrophils accumulated within the intima space (see Supplementary Fig. 2). IL-1β has a key function in the recruitment of neutrophils, and the IL-1-dependent intraperitoneal accumulation of neutrophils has frequently been used as an *in vivo* assay for inflammasome activation and IL-1 production[2,17,18]. Using this acute inflammation model we found that cholesterol crystals induced a robust induction of neutrophil influx into the peritoneum (Fig. 4a). Neutrophil influx into the peritoneum after deposition of cholesterol crystals was markedly decreased in mice lacking IL-1 or the IL-1 receptor (IL-1R), indicating that IL-1 production is indeed induced and essential for cholesterol-crystal-induced inflammation *in vivo*. Moreover, mice lacking NLRP3 inflammasome components or cathepsins B or L also recruited significantly fewer neutrophils into the peritoneum than wild-type mice after injection of cholesterol crystals. However, the decrease in neutrophilic influx observed after deposition of cholesterol crystals was more pronounced in mice lacking IL-1-related genes than in mice lacking NLRP3-inflammasome-related genes (Fig. 4a), presumably because of the contribution of IL-1α signalling and/or caspase-1-independent processing of IL-1β (ref. 19) *in vivo*. In any case, these data confirm that cholesterol crystals trigger NLRP3 inflammasome-dependent IL-1 production *in vivo*.

To test whether the NLRP3 inflammasome is involved in the chronic inflammation that underlies atherogenesis in vessel walls, we tested whether the absence of NLRP3, ASC or IL-1 cytokines might modulate atherosclerosis development in LDLR-deficient mice[20], a model for familial hypercholesterolaemia. We reconstituted lethally irradiated LDLR-deficient mice with bone marrow from wild-type or NLRP3-deficient, ASC-deficient or IL-1α/β-deficient mice and subjected these mice to eight weeks of a high-cholesterol diet. In these bone marrow chimaeras, the LDLR-deficiency radioresistant parenchyma causes the animals to become hypercholesterolaemic when placed on a high-fat diet, whereas their bone marrow-derived macrophages and other leukocytes lack the NLRP3-inflammasome or IL-1 pathway components needed to respond to cholesterol crystals. No significant differences in blood cholesterol levels were observed between the different groups (wild type, $893 \pm 144\ mg\ dl^{-1}$; *ASC*$^{-/-}$, $781 \pm 114\ mg\ dl^{-1}$; *Nlrp3*$^{-/-}$,$753 \pm 132\ mg\ dl^{-1}$; *Il1a*$^{-/-}$/*b*$^{-/-}$, $832 \pm 98\ mg\ dl^{-1}$). However, mice reconstituted with NLRP3-deficient, ASC-deficient or IL-1α/b-deficient bone marrow showed significantly lower plasma levels of IL-18, an IL-1 family cytokine whose secretion is dependent on inflammasomes and a biomarker known to be elevated in atherosclerosis[21] (Fig. 4b). Additionally, mice whose bone marrow-derived cells lacked NLRP3 inflammasome components or IL-1 cytokines were markedly resistant to the development of atherosclerosis (Fig. 4c, d). The lesional area in the aortae of these mice was decreased on average by 69% in comparison with chimaeric LDLR-deficient mice that had wild-type bone marrow. These data demonstrate that activation of the NLRP3 inflammasome by bone marrow-derived cells is a major contributor to diet-induced atherosclerosis in mice. However, the contribution of NLRP3 inflammasome activation in parenchymal cells to the development of atherosclerosis cannot be assessed with this disease model and remains to be examined in mice that are doubly deficient in both LDLR and inflammasome components.

The molecules that incite inflammation in atherosclerotic lesions have presented a long-standing puzzle. Although the lesions are absolutely dependent on cholesterol, this abundant, naturally occurring molecule has been viewed as inert. Here we show that the crystalline form of cholesterol can induce inflammation. The magnitude of the inflammatory response and the mechanism of NLRP3 activation seem identical to that of crystalline uric acid, silica and asbestos[2,3,22]. All these crystals are known to provoke clinically important inflammation as seen in gout, silicosis and asbestosis, respectively.

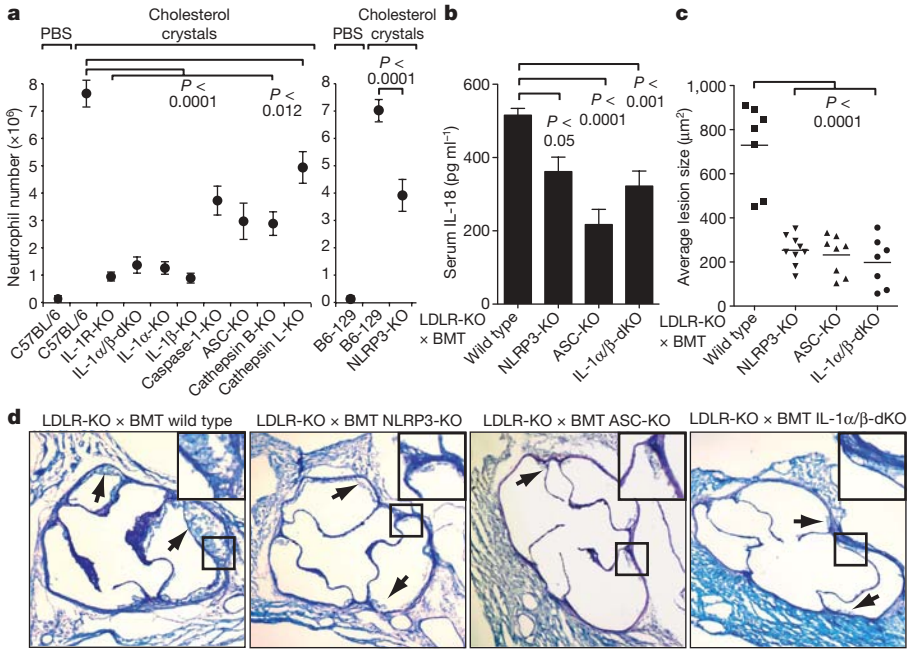

Figure 4 | The NLRP3 inflammasome mediates crystal-induced peritoneal inflammation and atherosclerosis *in vivo*. **a**, C57BL/6 ($n = 23$), B6-129 ($n = 13$) or mice deficient in genes encoding IL-1R ($n = 11$), IL-1α/β (double knockout, dKO; $n = 11$), IL-1α ($n = 4$), IL-1β ($n = 4$), caspase-1 ($n = 7$), ASC ($n = 15$), cathepsin B ($n = 10$), cathepsin L ($n = 5$) or NLRP3 ($n = 10$) were injected peritoneally with cholesterol crystals in PBS or with PBS alone (C57BL/6, $n = 14$; B6-129, $n = 4$). Peritoneal lavage cells were analysed for neutrophils after 15 h. Results are shown as means and s.e.m. for pooled groups of mice from experiments repeated two to four times. **b–d**, Female LDLR-KO mice reconstituted with C57BL/6 ($n = 7$), NLRP3-KO ($n = 9$), ASC-KO ($n = 8$) or IL-1α/β-dKO ($n = 7$) bone marrow were fed a high fat diet for 8 weeks and analysed for serum IL-18 concentration (**b**) and average aortic sinus lesion size (**c**, **d**). BMT, bone marrow transplantation. (**c**) Each dot represents the mean lesion size of serial cross-sections from individual mice. (**d**) Representative photographs of the aortic sinus stained with Giemsa. Insets show twofold magnified portions of the boxed images; arrows indicate atherosclerotic lesions.

The chronic inflammation in gout, silicosis and asbestosis is thought to derive from the inability of cells to destroy the ingested aggregates, leading to successive rounds of apoptosis and reingestion of the crystalline material[23]. In the same way, immune cells cannot degrade cholesterol; instead they depend on exporting the cholesterol to high-density lipoprotein (HDL) particles, which carry the cholesterol to the liver for disposal. The success of this or any cellular mechanism in clearing crystals may thus depend on the availability of HDL. A low concentration of HDL in the blood is one of the most prominent risk factors for atherosclerotic disease[24], and pharmacological methods of increasing HDL concentration are being actively pursued as treatments.

Even though cholesterol cannot be degraded by peripheral cells, it may be transformed to cholesteryl ester by the cellular enzyme acyl-coenzyme A:cholesterol acyltransferase (ACAT). Cholesteryl esters form droplets rather than crystals and are considered to be a storage form of cholesterol[4]. On the assumption that decreased cholesterol storage would be beneficial for decreasing atherosclerosis, ACAT inhibitors were tested in large clinical trials. Studies with two such inhibitors did not show a decrease but rather an increase in the size of the coronary atheroma[25,26]. This apparent paradox may be reconciled by our findings that the crystalline form of cholesterol, which would be expected to be increased in concentration after inhibition of ACAT, may be crucial in driving arterial inflammation. Indeed, mouse studies of ACAT deficiency show enhanced atherogenesis with abundant cholesterol crystals[27]. On the basis of our findings, therapeutic strategies that would reduce cholesterol crystals or block the inflammasome pathway would be predicted to have clinical benefit by decreasing the initiation or progression of atherosclerosis. In this context our findings also indicate novel molecular targets for the development of therapeutics to treat this disease.

METHODS SUMMARY

Cell culture media and reagents. Immortalized macrophage cell lines and bone marrow-derived cells were cultured as described[3] and primed with 10 ng ml^{-1} LPS for 2 h before the addition of inflammasome stimuli. Inhibitors were added 30 min before stimuli. Crystals and poly(dA-dT)•poly(dT-dA) were applied 6 h before supernatant was collected, and ATP (5 mM) and nigericin (10 μM) were applied 1 h before supernatant was collected. Poly(dA-dT)•poly(dT-dA) was transfected with Lipofectamine 2000 (Invitrogen). Human PBMCs were freshly isolated by Ficoll-Hypaque gradient centrifugation, grown in RPMI medium (Invitrogen), 10% FBS (Atlas Biologicals) 10 μg ml^{-1} ciprofloxacin (Celgro) at 2×10^5 cells per 96 wells, and primed with 50 pg ml^{-1} LPS for 2 h before the addition of inflammasome stimuli. Supernatants were assessed for IL-1β by enzyme-linked immunosorbent assay (ELISA) and western blotting.

Recruitment of neutrophils to peritoneal cavity. Mice were injected intraperitoneally with 2 mg of cholesterol crystals in 200 μl of PBS or with PBS alone. After 15 h, peritoneal lavage cells were stained with fluorescently conjugated monoclonal antibodies against Ly-6G (clone 1A8; Becton Dickinson) and 7/4 (Serotec) in the presence of monoclonal antibody 2.4G2 (FcgRIIB/III receptor blocker). The absolute number of neutrophils (Ly-6G-positive 7/4-positive) was determined by flow cytometry.

Bone marrow transplantation and atherosclerosis model. *Ldlr*$^{-/-}$ mice were irradiated and reconstituted with bone marrow from wild-type, *ASC*$^{-/-}$, *Nlrp3*$^{-/-}$ or *Il1a*$^{-/-}$*b*$^{-/-}$ mice. After 8 weeks of high-fat diet, the atherosclerotic regions of aortic sinuses were quantified on serially sectioned slides.

Full Methods and any associated references are available in the online version of the paper at www.nature.com/nature.

Received 25 June 2009; accepted 18 February 2010.

1. Wright, S. D. *et al.* Infectious agents are not necessary for murine atherogenesis. *J. Exp. Med.* **191,** 1437–1442 (2000).
2. Martinon, F., Petrilli, V., Mayor, A., Tardivel, A. & Tschopp, J. Gout-associated uric acid crystals activate the NALP3 inflammasome. *Nature* **440,** 237–241 (2006).
3. Hornung, V. *et al.* Silica crystals and aluminum salts activate the NALP3 inflammasome through phagosomal destabilization. *Nature Immunol.* **9,** 847–856 (2008).
4. Chang, T. Y., Chang, C. C., Ohgami, N. & Yamauchi, Y. Cholesterol sensing, trafficking, and esterification. *Annu. Rev. Cell Dev. Biol.* **22,** 129–157 (2006).
5. Small, D. M. George Lyman Duff memorial lecture. Progression and regression of atherosclerotic lesions. Insights from lipid physical biochemistry. *Arteriosclerosis* **8,** 103–129 (1988).
6. Stary, H. *et al.* A definition of advanced types of atherosclerotic lesions and a histological classification of atherosclerosis. A report from the Committee on Vascular Lesions of the Council on Arteriosclerosis, American Heart Association. *Arterioscler. Thromb. Vasc. Biol.* **15,** 1512–1531 (1995).
7. Abela, G. S. *et al.* Effect of cholesterol crystals on plaques and intima in arteries of patients with acute coronary and cerebrovascular syndromes. *Am. J. Cardiol.* **103,** 959–968 (2009).
8. Piedrahita, J. A., Zhang, S. H., Hagaman, J. R., Oliver, P. M. & Maeda, N. Generation of mice carrying a mutant apolipoprotein E gene inactivated by gene targeting in embryonic stem cells. *Proc. Natl Acad. Sci. USA* **89,** 4471–4475 (1992).
9. Zhang, S. H., Reddick, R. L., Piedrahita, J. A. & Maeda, N. Spontaneous hypercholesterolemia and arterial lesions in mice lacking apolipoprotein E. *Science* **258,** 468–471 (1992).
10. Martinon, F., Mayor, A. & Tschopp, J. The inflammasomes: guardians of the body. *Annu. Rev. Immunol.* **27,** 229–265 (2009).
11. Bauernfeind, F. G. *et al.* Cutting edge: NF-κB activating pattern recognition and cytokine receptors license NLRP3 inflammasome activation by regulating NLRP3 expression. *J. Immunol.* **183,** 787–791 (2009).
12. Hornung, V. *et al.* AIM2 recognizes cytosolic dsDNA and forms a caspase-1-activating inflammasome with ASC. *Nature* **458,** 514–518 (2009).
13. Stewart, C. R. *et al.* CD36 ligands promote sterile inflammation through assembly of a Toll-like receptor 4 and 6 heterodimer. *Nature Immunol.* **11,** 155–161 (2009).
14. Halle, A. *et al.* The NALP3 inflammasome is involved in the innate immune response to amyloid-β. *Nature Immunol.* **9,** 857–865 (2008).
15. Garin, J. *et al.* The phagosome proteome: insight into phagosome functions. *J. Cell Biol.* **152,** 165–180 (2001).
16. Yuan, X. M., Li, W., Olsson, A. G. & Brunk, U. T. The toxicity to macrophages of oxidized low-density lipoprotein is mediated through lysosomal damage. *Atherosclerosis* **133,** 153–161 (1997).
17. Chen, C. J. *et al.* Identification of a key pathway required for the sterile inflammatory response triggered by dying cells. *Nature Med.* **13,** 851–856 (2007).
18. Guarda, G. *et al.* T cells dampen innate immune responses through inhibition of NLRP1 and NLRP3 inflammasomes. *Nature* **460,** 269–273 (2009).
19. Dinarello, C. A. Immunological and inflammatory functions of the interleukin-1 family. *Annu. Rev. Immunol.* **27,** 519–550 (2009).
20. Ishibashi, S., Goldstein, J. L., Brown, M. S., Herz, J. & Burns, D. K. Massive xanthomatosis and atherosclerosis in cholesterol-fed low density lipoprotein receptor-negative mice. *J. Clin. Invest.* **93,** 1885–1893 (1994).
21. Blankenberg, S. *et al.* Interleukin-18 is a strong predictor of cardiovascular death in stable and unstable angina. *Circulation* **106,** 24–30 (2002).
22. Dostert, C. *et al.* Innate immune activation through Nalp3 inflammasome sensing of asbestos and silica. *Science* **320,** 674–677 (2008).
23. Mossman, B. T. & Churg, A. Mechanisms in the pathogenesis of asbestosis and silicosis. *Am. J. Respir. Crit. Care Med.* **157,** 1666–1680 (1998).
24. Gordon, T., Castelli, W. P., Hjortland, M. C., Kannel, W. B. & Dawber, T. R. High density lipoprotein as a protective factor against coronary heart disease. The Framingham Study. *Am. J. Med.* **62,** 707–714 (1977).
25. Nissen, S. E. *et al.* Effect of ACAT inhibition on the progression of coronary atherosclerosis. *N. Engl. J. Med.* **354,** 1253–1263 (2006).
26. Meuwese, M. C. *et al.* ACAT inhibition and progression of carotid atherosclerosis in patients with familial hypercholesterolemia: the CAPTIVATE randomized trial. *J. Am. Med. Assoc.* **301,** 1131–1139 (2009).
27. Accad, M. *et al.* Massive xanthomatosis and altered composition of atherosclerotic lesions in hyperlipidemic mice lacking acyl CoA:cholesterol acyltransferase 1. *J. Clin. Invest.* **105,** 711–719 (2000).

Supplementary Information is linked to the online version of the paper at www.nature.com/nature.

Acknowledgements This work was supported by grants from the National Institutes of Health (to E.L. and K.L.R.) and from the Deutsche Forschungsgemeinschaft (GK 1202, to M.S. and P.D.).

Author Contributions P.D., H.K., K.J.R, C.M.S., G.V., F.G.B, V.H., L.F. and E. Latz designed and performed experiments and analysed data. G.S.A. collected and prepared human samples. T.E., G.N., M.S., K.J.M., G.S.A., K.A.F. and E. Lien provided critical suggestions and discussions throughout the study. P.D., H.K., K.L.R., S.D.W., V.H. and E. Latz wrote the paper. E. Latz conceived and supervised the study.

Author Information Reprints and permissions information is available at www.nature.com/reprints. The authors declare no competing financial interests. Correspondence and requests for materials should be addressed to E.L. (eicke.latz@umassmed.edu; eicke.latz@uni-bonn.de).

METHODS

Mice. Mice were provided as follows: *Nlrp3*$^{-/-}$ and *ASC*$^{-/-}$ by Millennium Pharmaceuticals; *Casp1*$^{-/-}$ by R. Flavell; *Ctsb*$^{-/-}$ by T. Reinheckel; *Ctsl*$^{-/-}$ by H. Ploegh; and *Il1a*$^{-/-}$, *Il1b*$^{-/-}$ and *Il1a*$^{-/-}$*b*$^{-/-}$ by Y. Iwakura. B6-129 (mixed background), C57BL/*6*, *Il1r1*$^{-/-}$, *Apoe*$^{-/-}$ and *Ldlr*$^{-/-}$ mice were purchased from Jackson Laboratories. Animal experiments were approved by the University of Massachusetts and Massachusetts General Hospital Animal Care and Use Committees.

Reagents. Bafilomycin A1, cytochalasin D and zYVAD-fmk were from Calbiochem. ATP, acridine orange and poly(dA-dT)•poly(dT-dA) sodium salt were from Sigma-Aldrich, and ultra-pure LPS was purchased from InvivoGen. Nigericin, Hoechst dye, DQ ovalbumin and fluorescent choleratoxin B were purchased from Invitrogen. MSU crystals were prepared as described[17].

Cholesterol crystal preparation. Tissue-culture grade or synthetic cholesterol was purchased from Sigma, solubilized in hot acetone and crystallized by cooling. After six cycles of recrystallization, the final crystallization was performed in the presence of 10% endotoxin-free water to obtain hydrated cholesterol crystals. Cholesterol crystals were analysed for purity by electron impact gas chromatography–mass spectrometry and thin-layer chromatography with the use of silica gel and hexane-ethyl acetate (80:20) solvent. Crystal size was varied with a microtube tissue grinder. Fluorescent cholesterol was prepared by the addition of DiD or DiI dye (Invitrogen) in PBS.

ELISA and western blotting. ELISA measurements of IL-1β (Becton Dickinson) and IL-18 (MBL International) were made in accordance with the respective manufacturer's directions. Experiments for caspase-1 western blot analysis were performed in serum-free DMEM medium. After stimulations, cells were lysed by the addition of a 10× lysis buffer (10% Nonidet P40 in Tris-buffered saline (10 mM Tris-HCl, pH 7.5, 150 mM NaCl) and protease inhibitors), and post-nuclear lysates were separated by 4–20% reducing SDS–PAGE. Anti-mouse caspase-1 polyclonal antibody was provided by P. Vandenabeele. Anti-human cleaved IL-1β (Cell Signaling) from human PBMCs was analysed in serum-free supernatants as above without cell lysis.

Confocal microscopy. *Apoe*$^{-/-}$ mice maintained in a pathogen-free facility were fed with a Western-type diet (Teklad Adjusted Calories 88137; 21% (w/w) fat, 0.15% (w/w) cholesterol, 19.5% (w/w) casein; no sodium cholate) starting at 8 weeks of age; this continued for 2, 4, 8 or 12 weeks (three mice in each group). Mice were killed and hearts were collected as described[28]. Hearts were sectioned serially at the origins of the aortic valve leaflets, and every third section (5 μm thick) was stained with haematoxylin/eosin and imaged by light microscopy. Adjacent sections were fixed in 4% paraformaldehyde, blocked and permeabilized (10% goat serum and 0.5% saponin in PBS) and stained for 1 h at 37 °C with fluorescent primary antibodies against macrophages (MoMa-2; Serotec), dendritic cells (CD11c; Becton Dickinson) or neutrophils (anti-Neutrophil; Serotec) for imaging by confocal microscopy.

Human atherosclerotic lesions were obtained directly after autopsy, serially sectioned at 2–3-mm intervals, and frozen sections (5 mm thick) were prepared as above. Parallel sections were stained with Masson's trichrome stain. Tissues were prepared for microscopy as above. Macrophages were stained with anti-CD68 (Serotec); smooth muscle cells were revealed with fluorescent phalloidin (Invitrogen). Human and mouse samples were counterstained with Hoechst dye to reveal nuclei. The atherosclerotic lesions were imaged on a Leica SP2 AOBS confocal microscope where immunofluoroscence staining was revealed by standard confocal techniques, and crystals were observed with laser reflection using enhanced transmittance of the acousto-optical beam splitter as described[3]. Laser reflection and fluorescence emission occurs at the same confocal plane in this setup. The mean lesion area, amount of crystal deposition and monocyte marker presence were quantified from three digitally captured sections per mouse (Adobe Photoshop CS4 Extended). For quantification of the crystal mass and macrophages present, the sum of positive pixels (laser reflection and fluorescence, respectively) was determined and the area was calculated from the pixel size.

Confocal microscopy of mouse macrophages was performed as described[3]. DQ ovalbumin fluoresces only on proteolytic processing, marking phagolysosomal compartments in macrophages.

Acridine orange lysosomal damage assay. This assay was performed by flow cytometry as described[3].

Bone marrow transplantation and atherosclerosis model. Eight-week-old female *Ldlr*$^{-/-}$ mice were lethally irradiated (11 Gy). Bone marrow was prepared from femurs and tibiae of C57BL/6, *Nlrp3*$^{-/-}$, *ASC*$^{-/-}$ and *Il1a*$^{-/-}$*Il1b*$^{-/-}$ donor mice, and T cells were depleted with complement (Pel-Freez Biologicals) and anti-Thy1 monoclonal antibody (M5/49.4.1; American Type Culture Collection). Irradiated recipient mice were reconstituted with 3.5×10^6 bone marrow cells administered into the tail vein. After four weeks, mice were fed with a Western-type diet (Teklad Adjusted Calories 88137; 21% (w/w) fat, 0.15% (w/w) cholesterol, 19.5% (w/w) casein; no sodium cholate) for eight weeks. Mice were killed and perfused intracardially with formalin. Hearts were embedded in OTC (Optimal Cutting Temperature) (Richard-Allan Scientific) medium, frozen, and serially sectioned through the aorta from the origins of the aortic valve leaflets; every single section (10 μm thick) throughout the aortic sinus (800 μm) was collected. Quantification of average lesion area was performed from 12 sections stained with haematoxylin/eosin or Giemsa from each mouse by two independent investigators, with virtually identical results. Serum cholesterol levels were determined by enzymatic assay (Wako Diagnostics), and serum IL-18 was measured by SearchLight protein array technology (Aushon Biosystems).

Statistical analyses. The significance of differences between groups was evaluated by one-way analysis of variance (ANOVA) with Dunnett's post-comparison test for multiple groups to control group, or by Student's *t*-test for two groups. R^2 was calculated from the Pearson correlation coefficient. Analyses were performed with Prism (GraphPad Software, Inc.).

28. Moore, K. J. *et al.* Loss of receptor-mediated lipid uptake via scavenger receptor A or CD36 pathways does not ameliorate atherosclerosis in hyperlipidemic mice. *J. Clin. Invest.* **115**, 2192–2201 (2005).

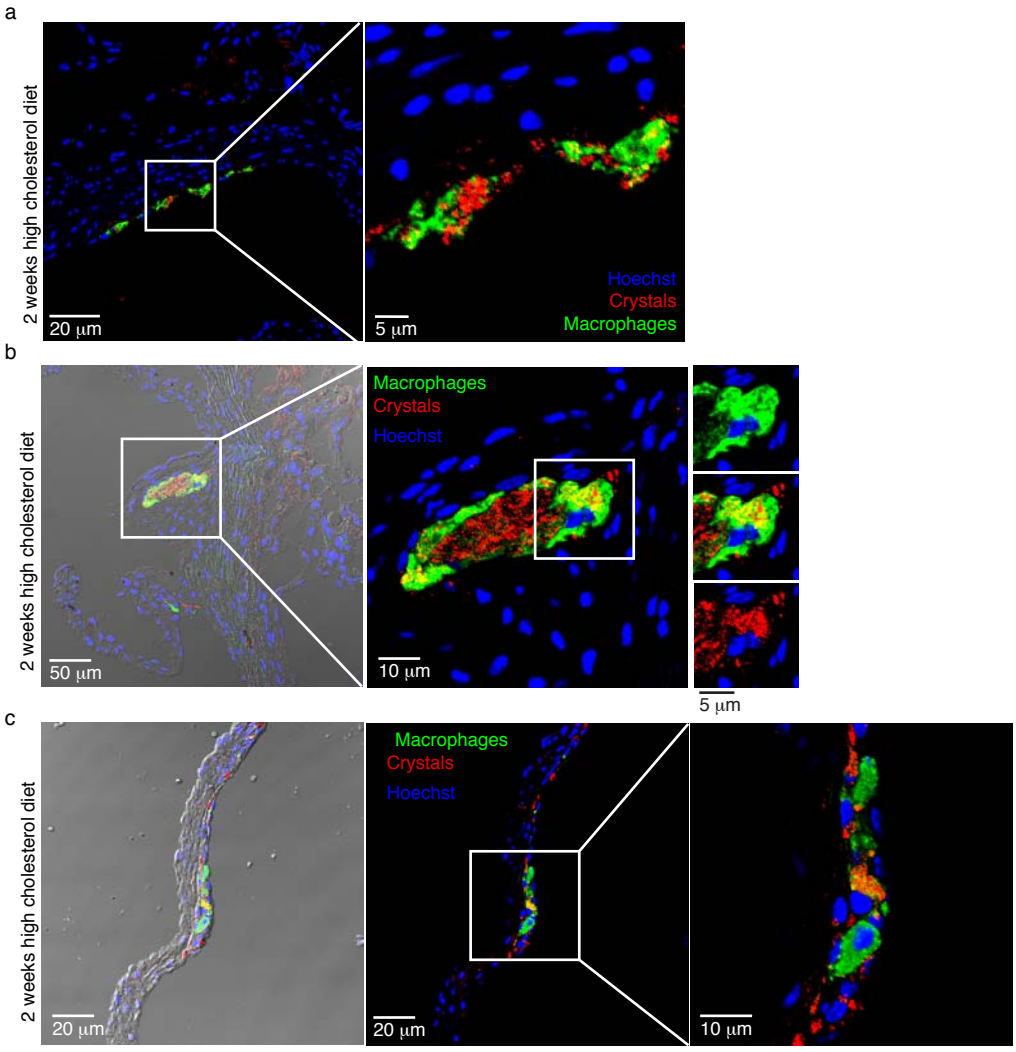

Supplementary Fig. 1: Early aortic sinus atherosclerotic lesions contain crystal-loaded macrophages.

a-c, Combined confocal fluorescence and reflection microscopy of early aortic sinus atherosclerotic lesions of Apo-E-KO mice fed a high cholesterol diet for 2 weeks. Laser reflection of cholesterol crystals (red), immunofluorescence of macrophages (green) identified by MoMa-2 and nuclei (blue) counterstained with Hoechst dye. Note: In early lesions individual subendothelial crystal-positive macrophages can be seen (a) and granuloma-like lesions of a few tens of macrophages encircling cholesterol crystal depositions are visible (b). Additionally, cholesterol-crystal positive macrophages can be found in leaflets of the heart valves (c). Representative images from serial sections of groups of 3 mice are shown.

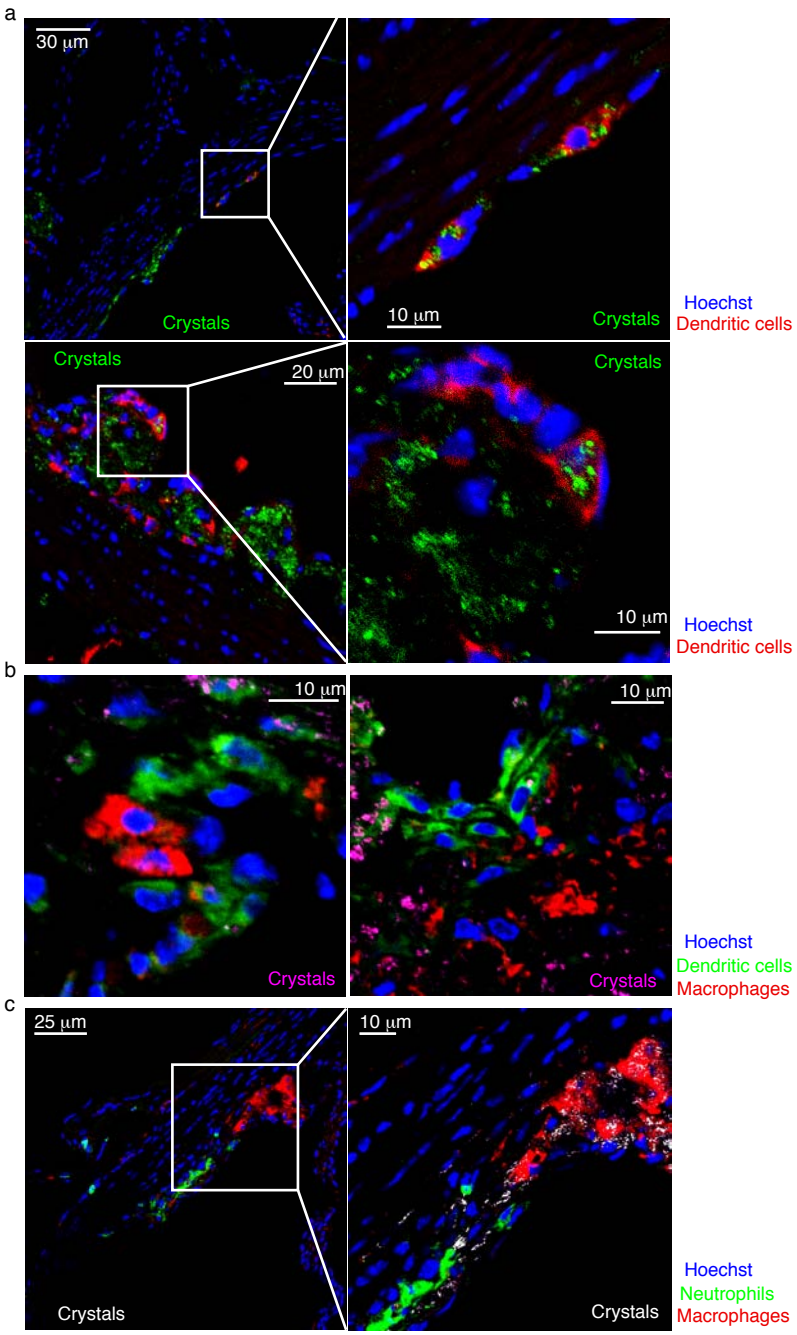

Supplementary Fig. 2: Early atherosclerotic lesions contain crystal-loaded macrophages at different sites of aortae.

a-c, Combined confocal fluorescence and reflection microscopy of early aortic sinus atherosclerotic lesions of Apo-E-KO mice fed a high cholesterol diet for 4 weeks. Samples were stained for (a) dendritic cells (CD11c, red), (b) macrophages (MoMa-2, red) and dendritic cells (CD11c, green) or (c) macrophages (MoMa-2, red) and neutrophils (anti-neutrophil, green). Nuclei were counterstained with Hoechst dye. Representative images from serial sections of groups of 3 mice are shown.

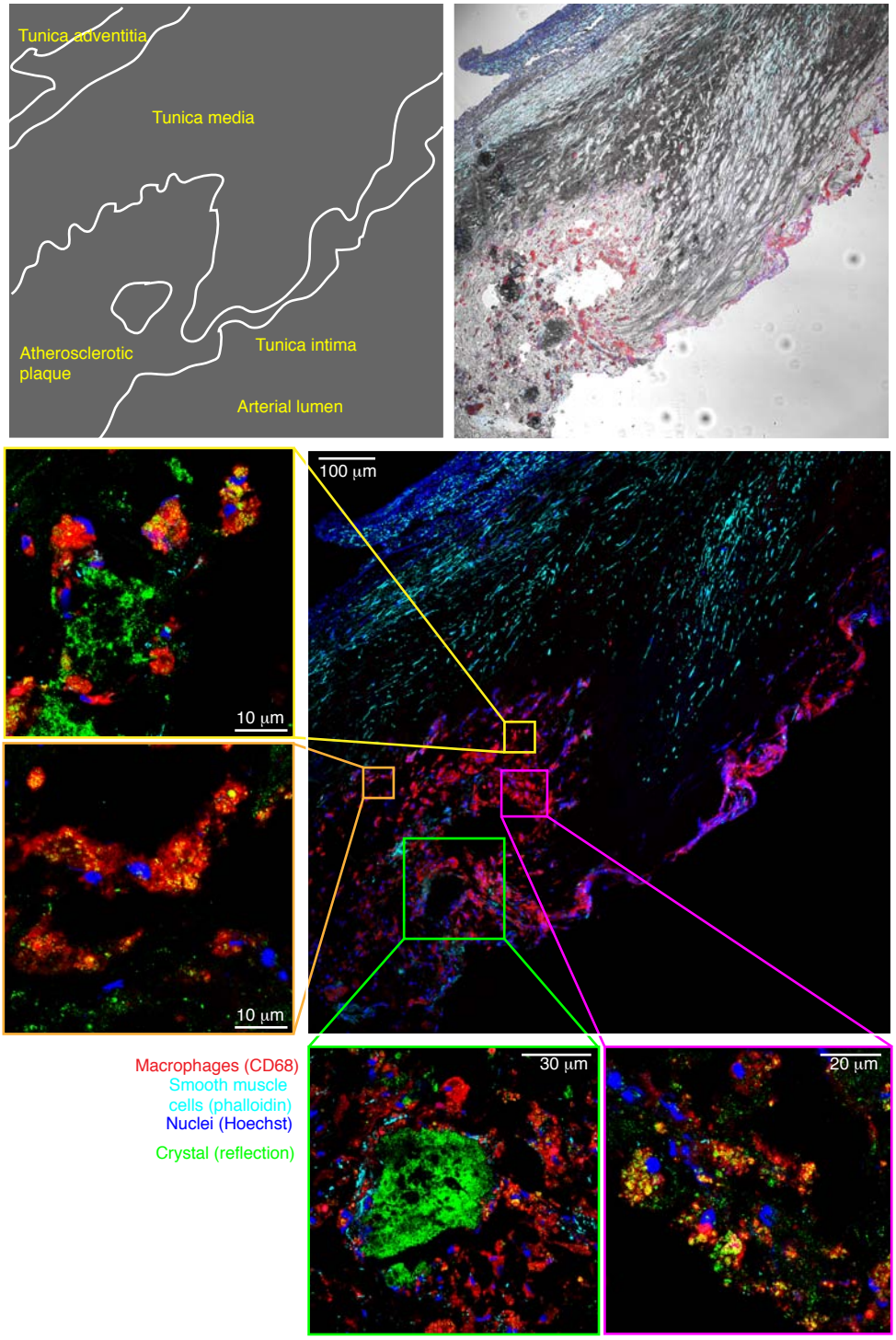

Supplementary Fig. 3: Human coronary artery atherosclerotic lesions contain crystals subendothelially and in necrotic cores.
Combined confocal fluorescence and reflection microscopy of a human coronary artery atherosclerotic lesion. Overview image was obtained without reflection microscopy, while magnifications of boxed areas were obtained using combined immunofluorescence and reflection detection. Tissue was stained for macrophages (CD68, red), smooth muscle cells (phalloidin, light blue) and nuclei (Hoechst dye, dark blue). A representative section of one patient is shown.

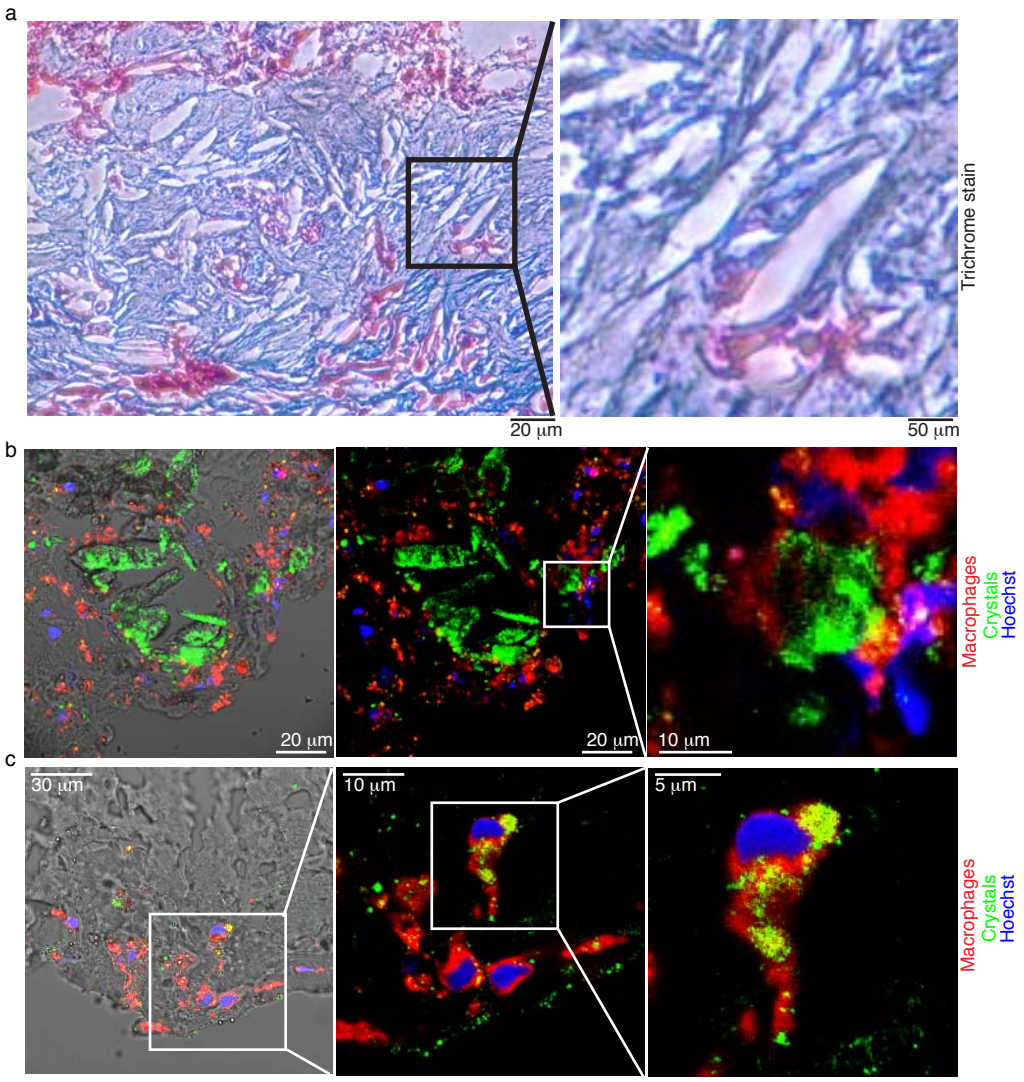

Supplementary Fig. 4: Human coronary artery lesion containing large cholesterol crystals a-c, Combined confocal fluorescence and reflection microscopy of a human coronary artery atherosclerotic lesion. Lesion was stained with Masson's trichrome stain (a). Note: Large cholesterol crystal clefts are visible, but small cholesterol crystals are not apparent. (b, c) Lesions were stained for macrophages (CD68, red). Note: Large cholesterol crystals are found extracellularly (b) and small crystals are found intracellularly (c). Sample imaged at 37 °C using a warmstage. Representative sections of two patients (b, c) (different from patient shown in Supplementary Fig. 3) are shown.

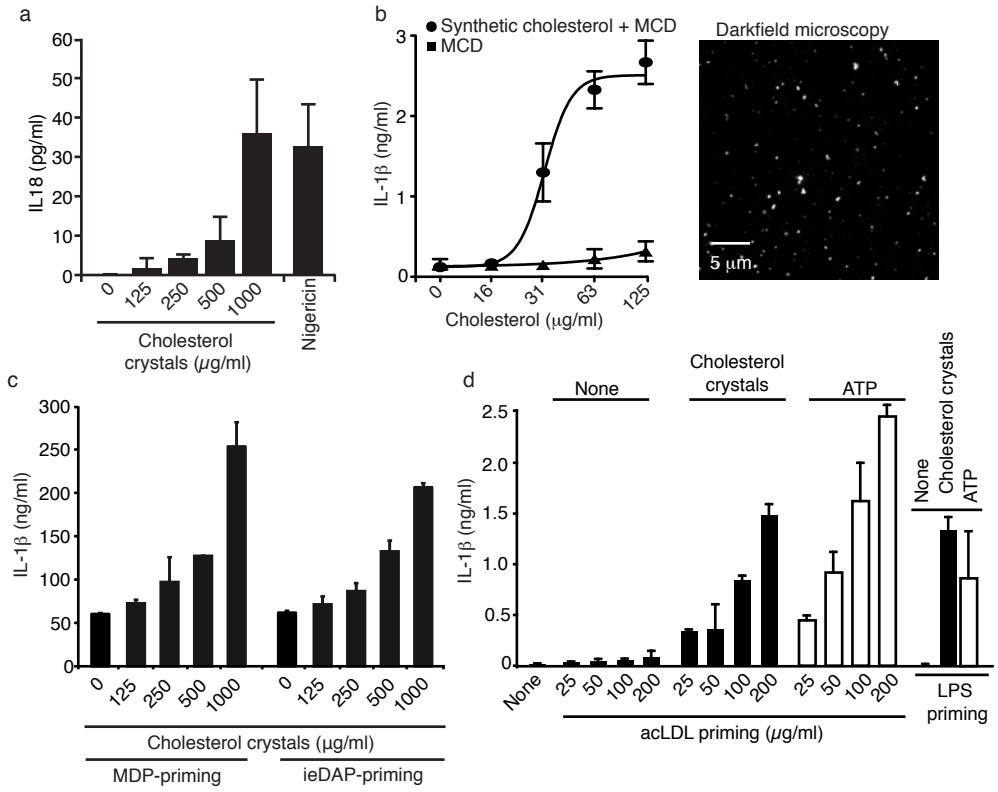

Supplementary Fig. 5: Cholesterol crystal-mediated IL-1β release in primary murine bone-marrow cells is dependent of the NLRP3 inflammasome.
a, IL-18 ELISA of supernatants from LPS-primed wild-type macrophages stimulated with cholesterol crystals or nigericin. **b,** IL-1β ELISA of supernatants from LPS-primed bone marrow derived DCs stimulated with synthetic cholesterol crystals with or without methylcyclodextrin (MCD). Equivalent doses of MCD were diluted into media of LPS-primed macrophages. Note: Upon dilution in aqueous culture media, small cholesterol crystals fall out of solution by dilution of the cholesterol-solubilizing agent MCD (b, right). **c, d,** IL-1β ELISA of supernatants from (c) MDP- or ieDAP- and (d) acetylated LDL- or LPS-primed mouse macrophages, stimulated with cholesterol crystals, ATP or left untreated. Means with s.e.m. from one out of two (a, c, d) three (b) representative experiments are shown.

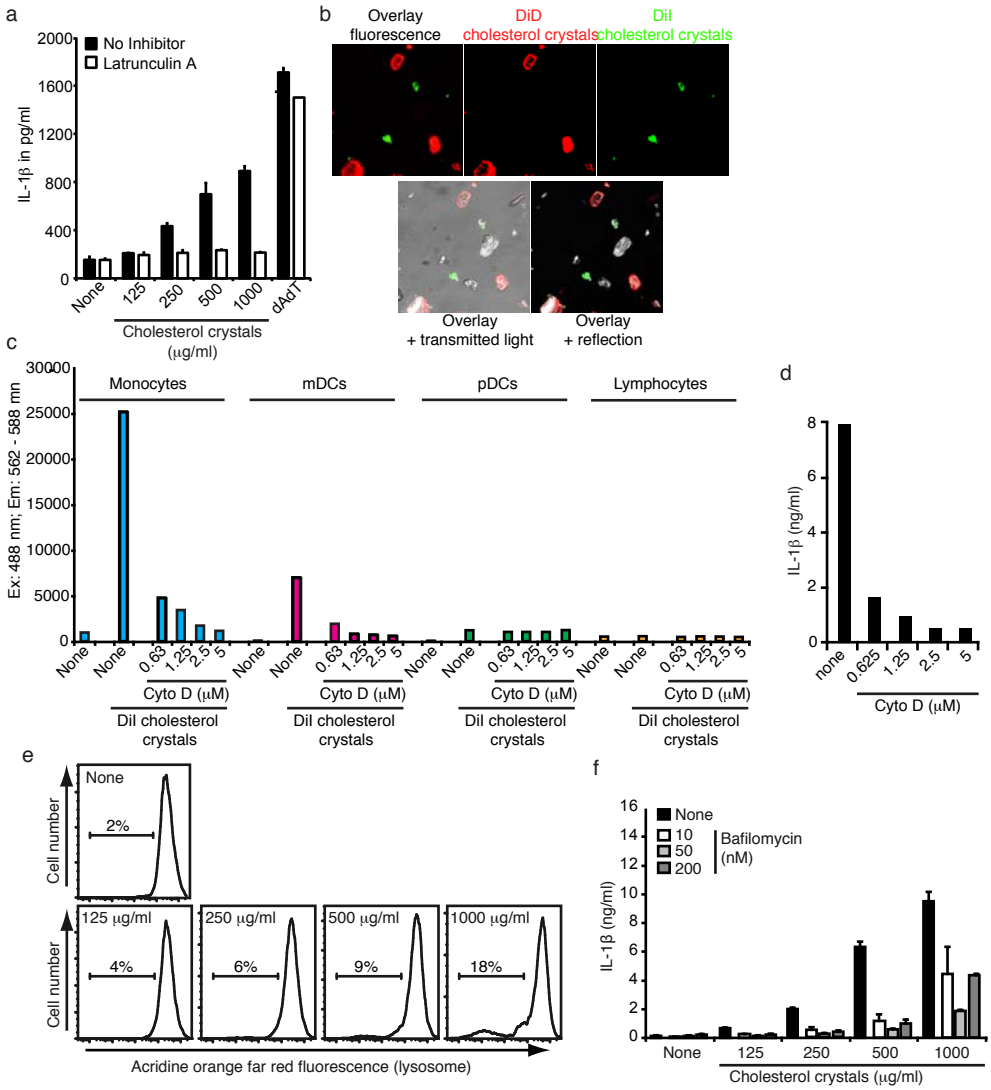

Supplementary Fig. 6: Fluorescent cholesterol crystals are phagocytosed by monocytes, macrophages and dendritic cells.

a, IL-1β ELISA of supernatants from LPS-primed mouse macrophages stimulated with cholesterol crystals or dAdT in the presence or absence of Latrunculin A. **b,** A mixture of unlabeled, DiI-labeled (green) or DiD-labeled (red) cholesterol crystals was incubated for 24 h and subsequently imaged by a combination of reflection (unlabeled, white) or fluorescence confocal imaging. Note: Dyes bound to the crystals do not exchange and non-labeled crystals do not acquire dye. **c,** PBMCs were incubated with DiI-labeled cholesterol crystals in the absence or presence of increasing amount of cytochalasin D. Cells were stained with surface markers to distinguish cell populations and analyzed by flow cytometry. The mean fluorescence intensity of DiI-cholesterol crystal uptake is shown for the different cell populations. **d,** LPS-primed human PBMCs were left untreated or treated with cytochalasin D and subsequently incubated with 250 μg/ml cholesterol crystals. IL-1β was determined in supernatants by ELISA. **e,** Murine macrophages stimulated with cholesterol crystals for 6h, stained with acridine orange and analyzed by FACS. **f,** IL-1β ELISA of supernatants from LPS-primed, murine macrophages stimulated with cholesterol crystals in the presence or absence of bafilomycin A1. Data are representative of one experiment repeated twice (a-d) or three times (e, f).

2.2 Originalarbeit: Bauer C., Duewell P., et al. *Gut* 2010

Colitis induced in mice with dextran sulfate sodium (DSS) is mediated by the NLRP3 inflammasome

Christian Bauer, Peter Duewell, Christine Mayer, Hans Anton Lehr, Kate A. Fitzgerald, Marc Dauer, Jurg Tschopp, Stefan Endres, Eicke Latz, and Max Schnurr

Gut doi:10.1136/gut.2009.197822

Colitis induced in mice with dextran sulfate sodium (DSS) is mediated by the NLRP3 inflammasome

Christian Bauer, Peter Duewell, Christine Mayer, et al.

Gut published online May 4, 2010
doi: 10.1136/gut.2009.197822

Gut Online First, published on May 4, 2010 as 10.1136/gut.2009.197822

Colitis induced in mice with dextran sulfate sodium (DSS) is mediated by the NLRP3 inflammasome

Christian Bauer,[1] Peter Duewell,[1] Christine Mayer,[1] Hans Anton Lehr,[2] Katherine A Fitzgerald,[3] Marc Dauer,[4] Jurg Tschopp,[5] Stefan Endres,[6] Eicke Latz,[3] Max Schnurr[1]

► Additional figures are published online only. To view these files please visit the journal online (http://gut.bmj.com).

[1]Department of Internal Medicine, University of Munich, Munich, Germany
[2]Institut Universitaire de Pathologie, Universite de Lausanne, Lausanne, Switzerland
[3]Department of Infectious Diseases and Immunology, University of Massachusetts Medical School, Worcester, Massachusetts, USA
[4]Department of Medicine II, Saarland University Hospital, Homburg/Saar, Germany
[5]Department of Biochemistry, University of Lausanne, Chemin des Boveresses 155, Epalinges, Switzerland
[6]Department of Clinical Pharmacology, University of Munich, Munich, Germany

Correspondence to
Dr Max Schnurr, Medizinische Klinik Innenstadt, University of Munich, Ziemssenstr. 1, D-80336 Munich, Germany; Max.Schnurr@med.uni-muenchen.de

CB and PD contributed equally to this work.

Revised 18 January 2010
Accepted 23 February 2010

ABSTRACT

Background The proinflammatory cytokines interleukin 1β (IL-1β) and IL-18 are central players in the pathogenesis of inflammatory bowel disease (IBD). In response to a variety of microbial components and crystalline substances, both cytokines are processed via the caspase-1-activating multiprotein complex, the NLRP3 inflammasome. Here, the role of the NLRP3 inflammasome in experimental colitis induced by dextran sodium sulfate (DSS) was examined.

Methods IL-1β production in response to DSS was studied in macrophages of wild-type, caspase-1$^{-/-}$, NLRP3$^{-/-}$, ASC$^{-/-}$, cathepsin B$^{-/-}$ or cathepsin L$^{-/-}$ mice. Colitis was induced in C57BL/6 and NLRP3$^{-/-}$ mice by oral DSS administration. A clinical disease activity score was evaluated daily. Histological colitis severity and expression of cytokines were determined in colonic tissue.

Results Macrophages incubated with DSS in vitro secreted high levels of IL-1β in a caspase-1-dependent manner. IL-1β secretion was abrogated in macrophages lacking NLRP3, ASC or caspase-1, indicating that DSS activates caspase-1 via the NLRP3 inflammasome. Moreover, IL-1β secretion was dependent on phagocytosis, lysosomal maturation, cathepsin B and L, and reactive oxygen species (ROS). After oral administration of DSS, NLRP3$^{-/-}$ mice developed a less severe colitis than wild-type mice and produced lower levels of proinflammatory cytokines in colonic tissue. Pharmacological inhibition of caspase-1 with pralnacasan achieved a level of mucosal protection comparable with NLRP3 deficiency.

Conclusions The NLRP3 inflammasome was identified as a critical mechanism of intestinal inflammation in the DSS colitis model. The NLRP3 inflammasome may serve as a potential target for the development of novel therapeutics for patients with IBD.

Significance of this study

What is known about this subject
- The proinflammatory cytokines IL-1β and IL-18 are central players in the pathogenesis of IBD.
- Activation and secretion of the IL-1 cytokine family is regulated by the NLRP3 inflammasome, a caspase-1-activating multiprotein complex.
- Single nucleotide polymorphisms (SNPs) in the NLRP3 gene region and other inflammasome-related genes are associated with susceptibility to Crohn's disease.

What are the new findings
- Using the acute dextran sodium sulfate (DSS) colitis model we found that NLRP3-deficient mice were significantly protected from colitis.
- We identified DSS as a stimulus of macrophage NLRP3 inflammasome activation in vitro and in vivo.
- IL-1β secretion was dependent on phagocytosis of DSS macromolecules, lysosomal maturation, cathepsin B and L, and reactive oxygen species (ROS).

How might this study impact on clinical practice
- The NLRP3 inflammasome complex may serve as a potential target for the development of novel therapeutics for patients with IBD.

INTRODUCTION

Human inflammatory bowel disease (IBD), the most important entities being ulcerative colitis and Crohn's disease, are chronic, relapsing and remitting inflammatory conditions that result from chronic dysregulation of the mucosal immune system in the gastrointestinal tract.[1] The precise pathogenesis of IBD is still incompletely understood. However, it is now widely accepted that genetic and environmental factors are involved. Animal models of experimental colitis have been developed to investigate the molecular and cellular mechanisms leading to IBD, and these models are frequently used to develop and evaluate the efficacy of novel anti-inflammatory drugs. In the acute dextran sodium sulfate (DSS) colitis model mice are fed with DSS polymers in the drinking water and this induces a colitis characterised by diarrhoea, bloody faeces, weight loss and a histological picture of inflammation and ulceration as seen in human IBD.[2] As the acute inflammatory response is independent of T and B cells,[3] the model is particularly useful to study the contribution of innate immune mechanisms in intestinal inflammation and, presumably due to toxic effects of DSS on the mucosa, epithelial barrier dysfunction.

Increased levels of proinflammatory cytokines, including interleukin-1β (IL-1β), IL-6, IL-18 and tumour necrosis factor α (TNFα), are detected in active IBD and correlate with the severity of inflammation.[4–6] IL-1β and TNFα have been shown to alter tight junctions and intestinal permeability.[7] As epithelial barrier integrity is essential for blocking the access of microorganisms and toxins to underlying tissues, IL-1β is likely to be essential in the early phase of the inflammatory

cascade leading to an inflamed colon. Indeed, enhanced levels of IL-1β are found in colonic mucosa and peritoneal macrophages in DSS-induced colitis and may hence represent an initial trigger of intestinal inflammation.[8] IL-1β and IL-18 are activated by caspase-1, and studies with caspase-1$^{-/-}$ mice strongly suggest that caspase-1 plays a key role in DSS-induced colitis.[9]

The NLR (nucleotide-binding domain and leucine-rich repeat-containing) family comprises a group of intracellular pattern recognition receptors. NLRs have a leucine-rich repeat (LRR) that recognises diverse pathogen-associated molecular patterns.[10] NOD2 and NLRP3 are two of the best characterised NLRs, and mutations of these receptors have been linked to Crohn's disease. NOD2 recognises the bacterial peptidoglycan-derived molecule muramyl dipeptide (MDP) and activates the nuclear factor-κB (NF-κB) pathway to induce an inflammatory response. Mutations of the NOD2 gene have been identified in individuals with Crohn's disease.[11 12] These polymorphisms have been linked to NF-κB activation and IL-1β secretion.[13] However, the exact interaction of NOD2, NF-κB and pro-IL-1β/IL-1β remains a matter of debate.[14] NLRP3, also known as cryopyrin, forms an inflammasome with the adaptor molecule ASC and caspase-1 to convert pro-IL-1β and pro-IL-18 into their active forms. Mutations in NLRP3 lead to chronic autoinflammatory syndromes.[15] Single nucleotide polymorphisms (SNPs) in the NLRP3 gene region are associated with susceptibility to Crohn's disease.[16] In addition, the combination of polymorphisms in NLRP3 and CARD8 was recently shown to be associated with Crohn's disease in Swedish male subjects.[17]

Recent studies have identified the autophagy protein Atg16L1 as a further susceptibility factor for Crohn's disease.[18 19] Notably, Atg16L1 deficiency causes Toll/IL-1 receptor domain-containing adaptor inducing interferon β (TRIF)-dependent activation of caspase-1, and mice lacking Atg16L1 in haematopoietic cells are highly susceptible to DSS-induced acute colitis.[20] Elevated systemic IL-1β and IL-18 levels in these mice correlated with severe mucosal inflammation, pointing towards an important role for deregulated caspase-1 activity in the pathogenesis of both IBD and DSS-induced colitis.[9]

In this study, we investigated the regulation of caspase-1 activation in response to DSS in murine macrophages with genetic deletions of NLRP3 inflammasome components. In addition, the role of the NLRP3 inflammasome in intestinal inflammation was investigated using the acute DSS colitis model.

METHODS

Cell culture and reagents

Macrophage cell lines of wild-type (WT), caspase-1$^{-/-}$, NLRP3$^{-/-}$, ASC$^{-/-}$, cathepsin B$^{-/-}$, cathepsin L$^{-/-}$ and IPAF$^{-/-}$ mice were generated as described.[21] Cells were cultured in Dulbecco's modified Eagle's medium (DMEM) high glucose supplemented with 1% L-glutamine (all PAA, Pasching, Austria), 10% fetal calf serum (FCS; GIBCO, Karlsruhe, Germany) and 10 μg/ml ciprofloxacin (Hexal, Holzkirchen, Germany). Human THP-1 cells were cultivated in RPMI supplemented with 10% FCS, 1% Na-pyruvate and 10 μg/ml ciprofloxacin, and differentiated with phorbol 12-myristate 13-acetate (PMA; 5 nM) 3 h before DSS stimulation. Primary human macrophages were generated from adherent peripheral blood mononuclear cells (PBMCs) of healthy donors and cultivated in RPMI with 2% AB serum (Lonza, Verviers, Belgium), 1% L-glutamine, 100 U/ml penicillin, 0.1 mg/ml streptomycin (PAA, Pasching, Austria) in the presence of 1000 U/ml recombinant human granulocyte-stimulating factor (rhGM-CSF; Berlex, Richmond, California, USA). The caspase-1 inhibitor z-YVAD-fmk, nigericin, cytochalasin D and bafilomycin A1 were purchased from Calbiochem (Darmstadt, Germany). Poly(dA:dT) sodium salt, *N*-acetyl-L-cysteine (NAC), ammonium pyrrolidinedithiocarbamate (APDC) and dextranase were from Sigma-Aldrich (Munich, Germany). All DSS reagents were from MP Biomedicals (Illkirch, France). Ultra pure lipolysaccharide (LPS) K12 and acridine orange were from Invitrogen (Toulouse, France). The caspase-1 inhibitor pralnacasan was provided by Sanofi-Aventis (Frankfurt, Germany). Cremophor EL was purchased from BASF (Ludwigshafen, Germany).

Speck formation assay

Assembly of the ASC-containing NLRP3 inflammasome was studied using macrophages that stably express the fusion protein ASC—cyan fluorescent protein (CFP). Cells were plated at a density of 10^6 cells/well, primed with 10 ng/ml LPS for 2 h and incubated with DSS for 24 h. The cells were washed and ASC—CFP speck formation was analysed by fluorescence microscopy (Zeiss, Jena, Germany) and ImageJ software (NIH, Bethesda, Maryland, USA) for digitally counting specks per high power field (HPF).

Flow cytometry

For the analysis of lysosomal damage macrophages were plated into 24-well culture dishes and stimulated for 24 h with DSS. The cells were washed and incubated with 1 μg/ml acridine orange for 15 min for staining of lysosomes. Cells were washed twice and fluorescence intensity was analysed at 600—650 nm emission wavelength with a FACSCanto II (BD Biosciences San Diego, California, USA). Data analysis was performed using FlowJo software (Tree Star, Ashland, Oregon, USA).

Mice

NLRP3$^{-/-}$ mice[22] were bred at the University of Munich and used for experiments between the ages of 8 and 16 weeks. Age-matched WT controls were purchased from Harlan Winkelmann (Borchen, Germany). Mice were fed standard mice chow pellets, had access to tap water supplied in bottles, and were acclimatised at least 7 days before they entered into experiments. All experiments were approved by the regional animal study committee and are in agreement with the guidelines for the proper use of animals in biomedical research.

Induction of colitis and treatment

Colitis was induced in C57BL/6 and NLRP3$^{-/-}$ mice with 2% DSS (molecular weight=40 kDa) dissolved in drinking water given ad libitum (days 1—9) as described.[2] Control mice were given tap water. The caspase-1 inhibitor pralnacasan was dissolved in 25% Cremophor EL solution and was filtered through syringe filters (0.2 μm). The substance was administered intraperitoneally at a dosage of 50 mg/kg body weight twice daily. Control animals received Cremophor EL intraperitoneally twice daily.

Clinical score and histological analysis

Body weight, the presence of occult or gross blood per rectum, and stool consistency were determined by two investigators blinded to the treatment groups. A scoring system was applied to assess diarrhoea and the presence of occult or overt blood in the stool.[23] Changes of body weight are indicated as loss of baseline body weight as a percentage. Postmortem, the colon was removed and pieces of colonic tissue were used for ex vivo analysis. For histology, rings of the transverse part of the colon were fixed in 4% buffered formalin and embedded in paraffin. Sections were stained with H&E according to standard

protocols. Histological scoring was performed in a blinded way by a pathologist (HAL). Focally increased numbers of inflammatory cells in the lamina propria were scored as 1, confluence of inflammatory cells extending into the submucosa as 2 and transmural extension of the infiltrate as 3. For tissue damage, discrete lymphoepithelial lesions were scored as 1, mucosal erosions as 2, and extensive mucosal damage and/or extension through deeper structures of the bowel wall as 3. The two equally weighted subscores (cell infiltration and tissue damage) were added and the combined histological colitis severity score ranged from 0 to 6.

Ex vivo analysis of colonic cytokines

Strips of colon were mechanically crushed, vortexed in 200 µl of Tissue Protein Extraction Reagent (Pierce, Rockford, USA) for 1 min and shock frozen in liquid nitrogen. The homogenate was centrifuged at 10 000 *g* at 4°C for 15 min. The amount of total extracted protein was determined by Bradford analysis using the BioRad Protein Assay (BioRad, Munich, Germany). The amount of IFNγ, IL-1β and TNFα in the colon homogenate was quantified by ELISA (BD Biosciences Pharmingen, San Diego, California, USA).

mRNA extraction and reverse transcription–PCR (RT–PCR)

Colonic tissue was cleaned in phosphate-buffered saline (PBS), snap-frozen in liquid nitrogen and stored at −70°C. Total cellular RNA was isolated by homogenising tissue with an Ultra Turrax instrument (Janke und Kunkel, Staufen im Breisgau, Germany) and using the Roche Total RNA Tissue Extraction Kit (Roche, Mannheim, Germany). The yield and purity of the RNA were determined by spectroscopic analysis and the concentration of total RNA was equilibrated. For reverse transcription, M-MLV reverse transcriptase (Gibco Life Technologies, Paisley, UK), RNase inhibitor (Roche), oligo(dT) primer for cDNA synthesis (Roche) and dNTP (Promega, Madison, Wisconsin, USA) were used. A Light Cycler Instrument (Roche) and the Light Cycler Fast Start DNA Master SYBR Green I Kit (Roche) were used for real-time PCR, according to the manufacturer's recommendations. Primers for murine glyceraldehyde phosphate dehydrogenase (GAPDH) and IP-10 (CXCL-10) were purchased as Light Cycler Primer Sets including standard DNA from Search-LC (Heidelberg, Germany). The number of copies in each sample was correlated with the number of GAPDH copies.

Isolation of peritoneal macrophages

Mice were sacrified by cervical dislocation under isoflurane anaesthesia, injected with 10 ml of PBS intraperitoneally and, after shaking, peritoneal lavage was performed. Collected peritoneal lavage fluid was centrifuged and erythrocytes in the cell pellet were lysed using BD Pharm Lyse lysing buffer (BD Bioscience). The remaining cells were plated into culture dishes overnight and adherent cells were used for cytokine assays.

ELISA

Primary macrophages and cell lines were seeded into 96-well plates at a density of 2×10^5 cells per well. After LPS priming for 1 h, cells were stimulated with the indicated amounts of DSS for 24 h. Cell culture supernatant or colon homogenates were used for ELISAs (BD Bioscience), which were performed according to the manufacturer's protocol.

SDS–PAGE and western blotting

Cell culture supernatants of 10^6 cells or 65 µg of whole protein from colon homogenate were dissolved in Laemmli buffer (BioRad) and separated using a 15% acrylamide–bisacrylamide gel. Proteins were blotted onto a 0.45 µm polyvinylidene fluoride (PVDF) membrane (Millipore, Schwalbach, Germany). Primary anti-caspase-1 (rabbit, antimouse, Santa Cruz) and anti-IL-1β (R&D Systems, Wiesbaden-Nordenstadt, Germany) were applied at 1:500 and horseradish peroxidase (HRP)-coupled ß-actin (loading control) was used at 1:3000. Immunoglobulin G (IgG) antigoat-HRP (Santa Cruz) was diluted 1:3000 and Amersham ECL™ (GE Healthcare, Munich, Germany) served for visualisation via chemoluminescence.

Statistical analysis

Data are expressed as means ± SEM. Statistical significance of differences between treatment and control groups was determined by Student t test. Differences were considered statistically significant at $p<0.05$.

RESULTS

DSS induces caspase-1-dependent IL-1β processing in murine macrophages

Release of active IL-1β is mediated by a two-step process initiated by transcriptional induction of pro-IL-1β, for example by a Toll-like receptor (TLR) stimulus, followed by caspase-1-mediated cleavage. DSS, a polyanionic derivate of sulfated high molecular weight dextrane, induces the release of IL-1β from murine macrophages.[8] To investigate the mechanism of IL-1β release, we incubated a murine macrophage cell line with DSS for 24 h with or without prior LPS priming. In the absence of LPS priming, DSS did not induce a notable release of IL-1β. However, LPS-primed macrophages strongly responded to the addition of DSS in a dose-dependent manner (figure 1A). The requirement of LPS priming for enhanced IL-1β synthesis was further supported by data obtained from a macrophage cell line of mice with combined MyD88 and TRIF deficiency. These cells failed to secrete IL-1β in response to either DSS or nigericin, a potassium ionophore activating caspase-1, but responded to poly(dA:dT), which induces IL-1β in a TLR-independent manner (figure 1B). To demonstrate the role of caspase-1 in DSS-mediated IL-1β release, we incubated the macrophages with the caspase-1 inhibitor z-YVAD-fmk and found that this completely abolished the release of IL-1β (figure 1C). Similar results were obtained using primary peritoneal macrophages from WT mice (figure 1D) as well as primary human macrophages and THP-1 cells (Supplementary figure 1). To confirm that IL-1β is released in its active form, we performed western blotting of IL-1β p17 and caspase-1 p10, which were both present in supernatants of DSS- or nigericin-stimulated macrophages (figure 1E). To determine whether intact DSS macromolecules were required for caspase-1 activation, we digested DSS (40 kDa) with dextranase, which cleaves 1,6-glycosylic bounds of isomaltose, before macrophage stimulation. Dextranase almost completely inhibited the release of IL-1β (figure 1F). Incubating macrophages with DSS molecules ranging from 8 to 1400 kDa revealed a positive correlation between IL-1β release and DSS molecular weight (figure 1G), suggesting that IL-1β secretion is induced only by intact DSS macromolecules.

DSS induces NLRP3 inflammasome activation

The NLR protein NLRP3 can form an inflammasome complex with the adaptor molecule ASC and caspase-1 in response to various stimuli.[24] We speculated that caspase-1 activation by DSS is mediated by the NLRP3 inflammasome. It has been shown that NLRP3 inflammasome activation is dependent

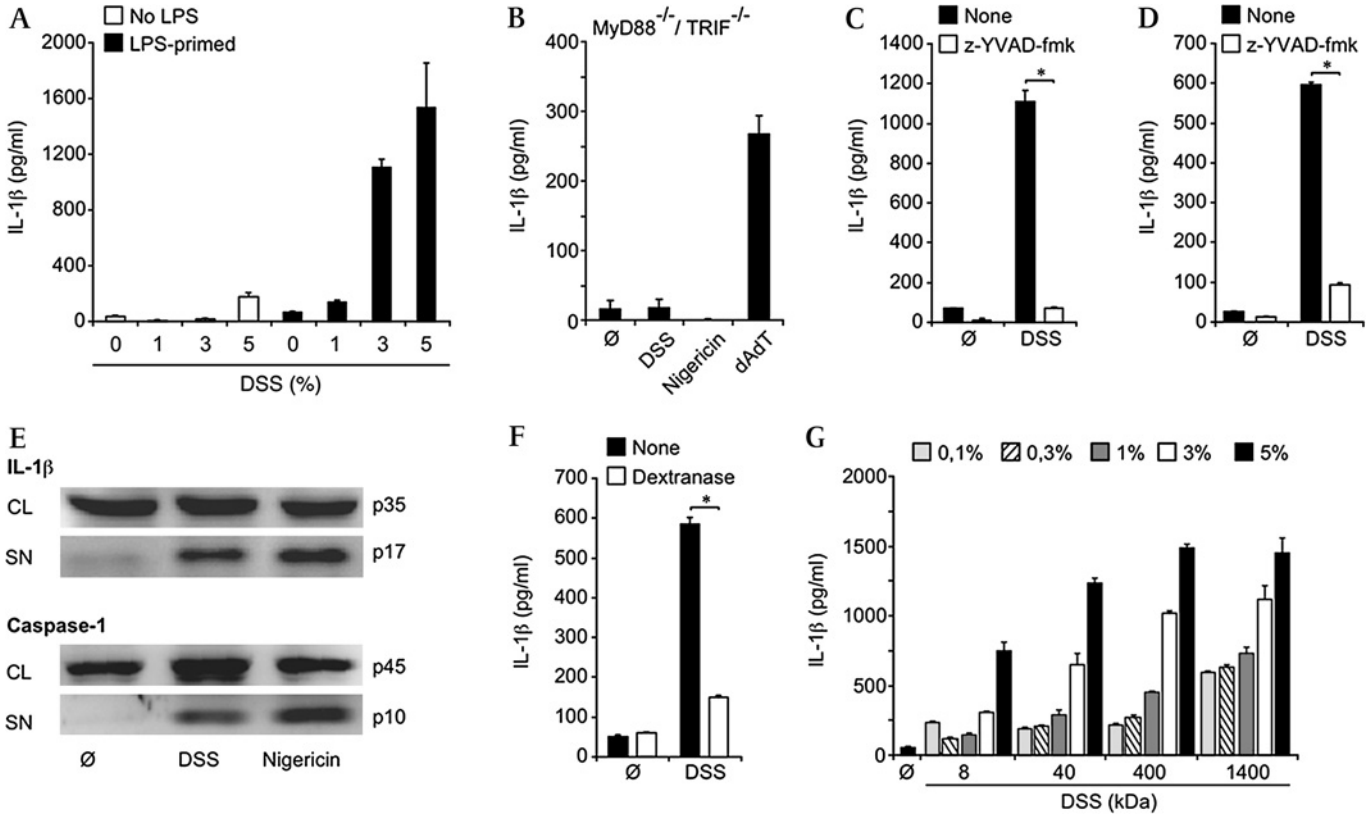

Figure 1 Dextran sodium sulfate (DSS) induces caspase-1-mediated interleukin 1β (IL-1β) release from murine macrophages. (A) Macrophages were treated with increasing concentrations of DSS in the absence or presence of lipopolysaccharide (LPS) priming. IL-1β was determined in the supernatant by ELISA. (B) Absence of IL-1β release of LPS-primed MyD88/TRIF-deficient macrophages in response to DSS or nigericin. Transfected dAdT served as a MyD88/TRIF-independent stimulus. (C) Influence of the caspase-1 inhibitor z-YVAD-fmk (10 μM) on IL-1β release by a macrophage cell line and (D) by primary macrophages. (E) Western blot analysis of IL-1β p35 and caspase-1 p45 in cell lysates (CL) and of bioactive IL-1β p17 and caspase-1 p10 in supernatants (SN) of DSS- or nigericin-stimulated, LPS-primed macrophages. (F) Influence of dextranase treatment of DSS on IL-1β release by macrophages. (G) Influence of DSS molecule size (8 to 1400 kDa) on IL-1β release. Shown are representative data as means ± SEM (n=3 independent experiments). *$p<0.05$. TRIF, Toll/IL-1 receptor domain-containing adaptor inducing interferon β.

on K^+ efflux.[25] To assess the role of NLRP3 in DSS-induced caspase-1 activation, we blocked K^+ efflux by the addition of high concentrations of KCl to the extracellular medium and found that this completely inhibited IL-1β release (figure 2A). In addition, macrophages lacking NLRP3, ASC or caspase-1 were devoid of IL-1β secretion in response to DSS exposure (figure 2B). Consistent with previous observations,[21] response to transfected poly(dA:dT) was NLRP3 independent and ASC dependent. In contrast, macrophages from $IPAF^{-/-}$ mice (IPAF is an NLRP3-independent, caspase-1-recruiting inflammasome) showed no defect in IL-1β secretion (figure 2C). The requirement of NLRP3 for IL-1β release was further supported by studying primary peritoneal macrophages from $NLRP3^{-/-}$ mice (figure 2D). NLRP3 activation triggers the formation of a large assembly of ASC, which rapidly activates caspase-1. To analyse the recruitment of ASC, we used macrophages stably expressing ASC fused to the fluorescent protein CFP.[26] NLRP3—ASC assembly results in the formation of fluorescent specks, which can be visualised by fluorescence microscopy. DSS induced speck formation in a dose-dependent manner (figure 2E). We could rule out that DSS, either directly or indirectly, induces NLRP3 inflammasome activation via the P2X7 receptor[27] by demonstrating that IL-1β secretion in response to DSS was unimpaired in macrophages lacking P2X7 (figure 2F). Together, these findings indicate that DSS activates the NLRP3—ASC complex, leading to the activation of caspase-1 and subsequent cleavage of pro-IL-1β into the mature, secreted form.

NLRP3 inflammasome activation in response to DSS is dependent on lysosomal maturation and reactive oxygen species (ROS)

Phagocytosis of particulate danger-associated molecular patterns has been shown to activate the NLRP3 inflammasome via lysosomal destabilisation.[21] To characterise the mechanisms of NLRP3 inflammasome activation in response to DSS further, we used pharmacological inhibitors to block pathways of lysosome formation and function. The role of phagosome formation in caspase-1 activation was studied by incubating macrophages prior to DSS stimulation with cytochalasin D, which inhibits phagocytosis by disrupting actin filaments. Cytochalasin D completely abrogated IL-1β secretion in response to DSS, whereas the response to the potassium ionophore nigericin was unaffected (figure 3A). Moreover, blocking lysosomal acidification with bafilomycin A1, an inhibitor of the vacuolar H^+ ATPase, completely inhibited DSS-mediated IL-1β release (figure 3A). These findings suggest a critical role for functional lysosomes in DSS-mediated NLRP3 activation. Experiments using specific inhibitors of cathepsin B have shown a link between lysosomal cysteine proteinases and NLRP3 inflammasome activation for crystals and influenza virus.[21 28] To assess whether this mechanism is operative during DSS-mediated NLRP3 inflammasome

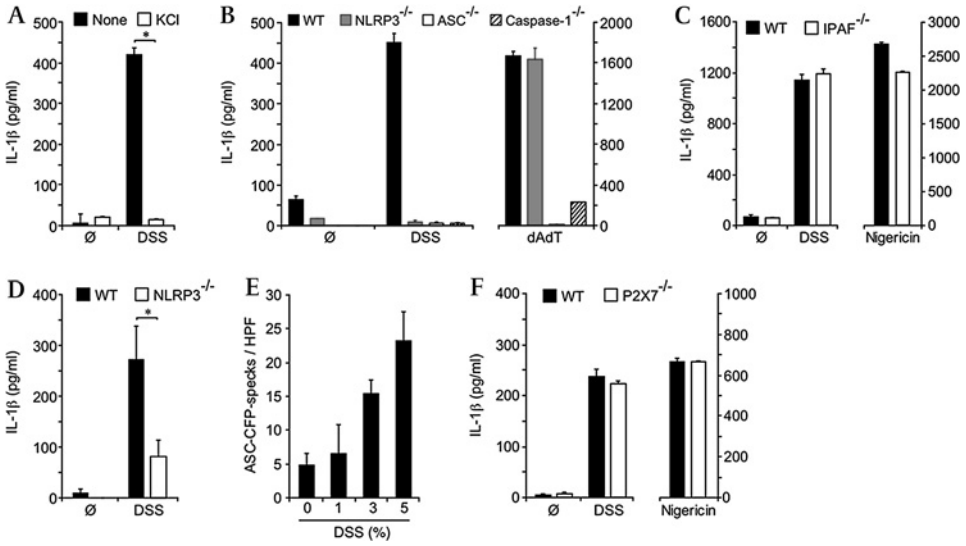

Figure 2 Interleukin 1β (IL-1β) processing in response to dextran sodium sulfate (DSS) is mediated by the NLRP3 inflammasome. (A) Macrophages were primed with lipopolysaccharide (LPS) and incubated with 3% DSS in the presence or absence of high concentrations of KCl (130 mM). IL-1β was determined in the supernatant by ELISA. (B) LPS-primed macrophage cell lines from wild-type (WT), NLRP3$^{-/-}$, ASC$^{-/-}$ or caspase-1$^{-/-}$ mice were incubated with 3% DSS. Incubation with dAdT served as a NLRP3-independent, but ASC-dependent stimulus. (C) IL-1β secretion by macrophages deficient in the IPAF inflammasome. (D) IL-1β secretion in response to 3% DSS by primary macrophages from WT and NLRP3$^{-/-}$ mice. (E) Recruitment of ASC to the inflammasome was visualised using macrophages expressing an ASC—cyan fluorescent protein (CFP) fusion protein by fluorescence microscopy. The numbers of specks per high power field (HPF) were counted. (F) IL-1β secretion by macrophages deficient in the P2X7 receptor. Shown are representative data as means ± SEM (n=3 independent experiments). *p<0.05.

activation, we compared IL-1β release of the WT with that of cathepsin B- and cathepsin L-deficient macrophages. IL-1β secretion in DSS-treated macrophages was significantly reduced in cathepsin B- and, to a lesser extent, in cathepsin L-deficient macrophages (figure 3B). Thus, lysosomal proteases appear to be involved in DSS-induced NLRP3 inflammasome activation. We next assessed whether DSS leads to lysosomal damage, as has been proposed for crystalline structures.[21] We made use of the staining properties of acridine orange, a dye with green fluorescence in its monomeric state and red fluorescence when forming dimers in acidic compartments, the red fluorescence intensity correlating with the cytoplasmic number of lysosomes. Indeed, DSS induced a loss of red fluorescence of macrophages stained with acridine orange at similar levels to those previously reported for crystals,[21] suggesting lysosomal damage (figure 3C). Taken together, these findings point towards a DSS-mediated phagosomal destabilisation, leading to the release of phagosomal contents into the cytosol where they are sensed by the NLRP3 inflammasome.

NLRP3 inflammasome activation has been linked with ROS generation in response to various stimuli.[28 29] DSS has previously been shown to stimulate macrophage ROS production.[30] To investigate the role of ROS in DSS-induced IL-1β release, we treated macrophages with the ROS inhibitors *N*-acetylcysteine (NAC) and ammonium pyrrolidinedithiocarbamate (APDC). Both inhibitors significantly reduced IL-1β secretion (figure 3D). These data suggest that ROS contribute to DSS-induced NLRP3 inflammasome activation.

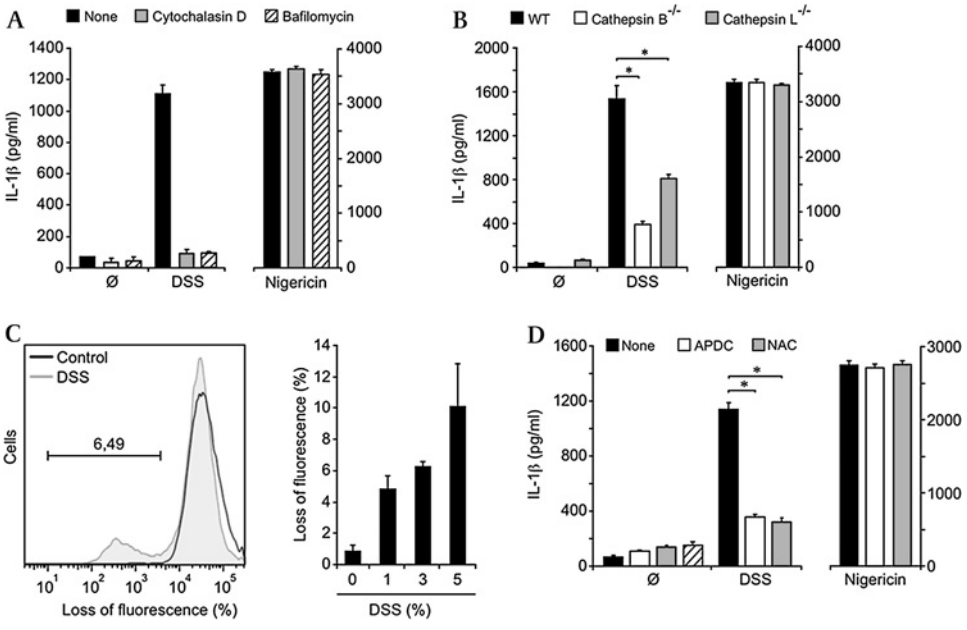

Figure 3 Activation of the NLRP3 inflammasome by dextran sodium sulfate (DSS) requires lysosomal maturation and reactive oxygen species (ROS). (A) Macrophages were incubated with cytochalasin D (2 μM) or bafilomycin A1 (20 nM) before treatment with 3% DSS. The potassium ionophore nigericin served as positive control. Interleukin 1β (IL-1β) was determined by ELISA. (B) Macrophage cell lines from wild-type (WT), cathepsin B$^{-/-}$ or cathepsin L$^{-/-}$ mice were primed with lipopolysaccharide (LPS) and incubated with DSS. (C) Phagosomes of DSS-treated macrophages were stained with the fluorochrome acridine orange. Loss of fluorescence, which correlates with reduced numbers of lysosomes, was analysed by fluorescence-activated cell sorting. (D) Influence of the ROS inhibitors, ammonium pyrrolidinedithiocarbamate (APDC) and *N*-acetyl-L-cysteine (NAC), on DSS-induced IL-1β production. Nigericin served as a positive control. Shown are representative data as means ± SEM (n=3 independent experiments). *p<0.05.

Colitis severity and inflammatory response in the DSS model depend on NLRP3 signalling

We next investigated the role of the NLRP3 inflammasome in DSS-mediated intestinal inflammation in vivo. WT and NLRP3$^{-/-}$ mice received 2% DSS in their drinking water for a period of 9 days. Clinical parameters, including body weight, the presence of occult or gross blood per rectum and stool consistency, were determined daily. NLRP3$^{-/-}$ mice were significantly protected from DSS-induced colitis, showing reduced loss of body weight and haematochezia (figure 4A). Of note, four out of 15 WT mice had died due to colitis by day 9, whereas all 15 NLRP3$^{-/-}$ mice survived. Histological analysis of colonic tissue obtained on day 6 revealed less severe mucosal infiltration by inflammatory cells and reduced tissue damage in NLRP3$^{-/-}$ mice, translating into a significantly improved histological colitis severity score (figure 4B and Supplementary figure 2). On day 9, histology showed severe intestinal inflammation with destruction of the epithelial layer leading to identical histology scores in WT and NLRP3$^{-/-}$ mice, despite the reduced clinical colitis scores in NLRP3$^{-/-}$ mice. These findings indicate that the NLRP inflammasome plays a more critical role during the early phase of colitis induction, but cannot prevent colitis progression after prolonged DSS exposure. As caspase-1 activity is regulated by NLRP3, inhibition of caspase-1 could be an effective novel treatment strategy for IBD. In line with this notion, we have previously reported that pharmacological inhibition of caspase-1 with pralnacasan is effective in the treatment of DSS-induced experimental colitis.[23] Treatment of mice with pralnacasan, at a dose that had been optimal in our previous study, improved clinical parameters, such as body weight, stool consistency and haematochezia (figure 4C). Indeed, the magnitude of the therapeutic benefit was similar to the protective effect observed in NLRP3$^{-/-}$ mice, providing further evidence that caspase-1 activation via the NLRP3 inflammasome is a major pathological mechanism in DSS-induced colitis.

Proinflammatory cytokines, including IL-1β, TNFα and IFNγ, are elevated in colonic tissue in humans and in the acute DSS colitis model. To assess the influence of the NLRP3 inflammasome on the intestinal inflammatory response, we first analysed IL-1β production of peritoneal macrophages isolated from mice receiving DSS in their drinking water. Macrophages of WT mice spontaneously released low levels of IL-1β, which was strongly enhanced by DSS feeding. In contrast, macrophages of NLRP3$^{-/-}$ mice secreted no detectable levels of IL-1β in the absence of DSS feeding and only low levels in response to DSS (figure 5A). Furthermore, levels of TNFα, IFNγ and IP-10 in colonic homogenates were elevated in WT but not in NLRP3$^{-/-}$ mice in response to 6 days of DSS feeding (figure 5B). Interestingly, levels of these cytokines were also reduced in NLRP3$^{-/-}$ mice receiving tap water only, indicating that NLRP3 might also play a role in physiological intestinal homeostasis. Of interest, IL-1β levels in colonic homogenates measured by ELISA did not differ significantly between WT and NLRP3$^{-/-}$ mice. As the ELISA does not discriminate between pro-IL-1β and active IL-1β, we performed western blot analysis for cleaved IL-1β (p17) and found high levels of cleaved IL-1β in the colon of WT mice receiving DSS, but not in that of NLRP3$^{-/-}$ mice (figure 5C).

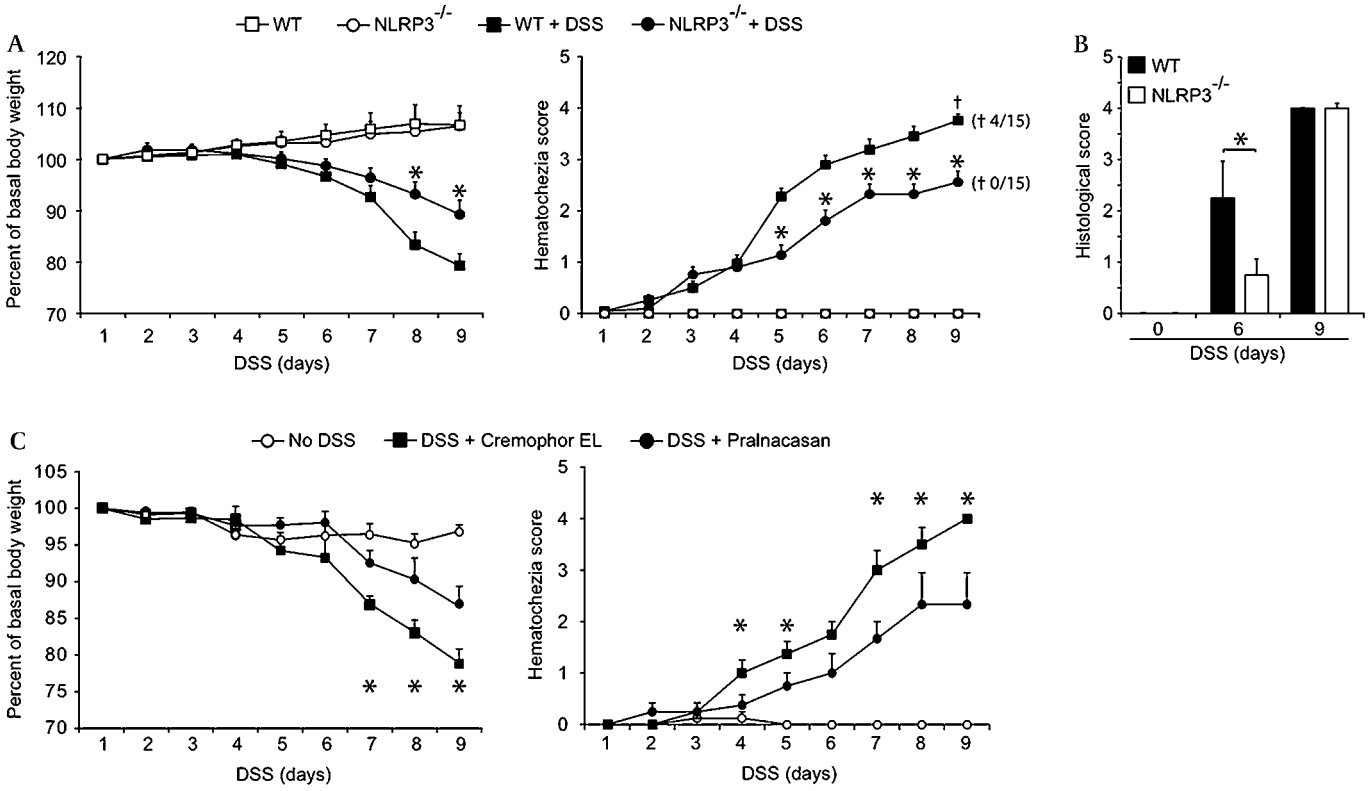

Figure 4 NLRP3 deficiency and caspase-1 inhibition protects mice from dextran sodium sulfate (DSS)-induced colitis. (A) Loss of basal body weight and haematochezia score of wild-type (WT) and NLRP3$^{-/-}$ mice (n=15 per group) receiving 2% DSS or tap water for 9 days. † indicates death rate. (B) Histological score of distal colon sections of WT and NLRP3$^{-/-}$ mice receiving DSS or tap water on day 6 and day 9 of DSS feeding. (C) Loss of basal body weight and haematochezia score of WT mice treated with tap water or 2% DSS orally ad libitum in the presence or absence of the caspase-1-inhibitor pralnacasan (50 mg/kg intraperitoneally) or with Cremophor EL (vehicle) alone. Data are presented as means ± SEM (n=2 independent experiments). *$p<0.05$.

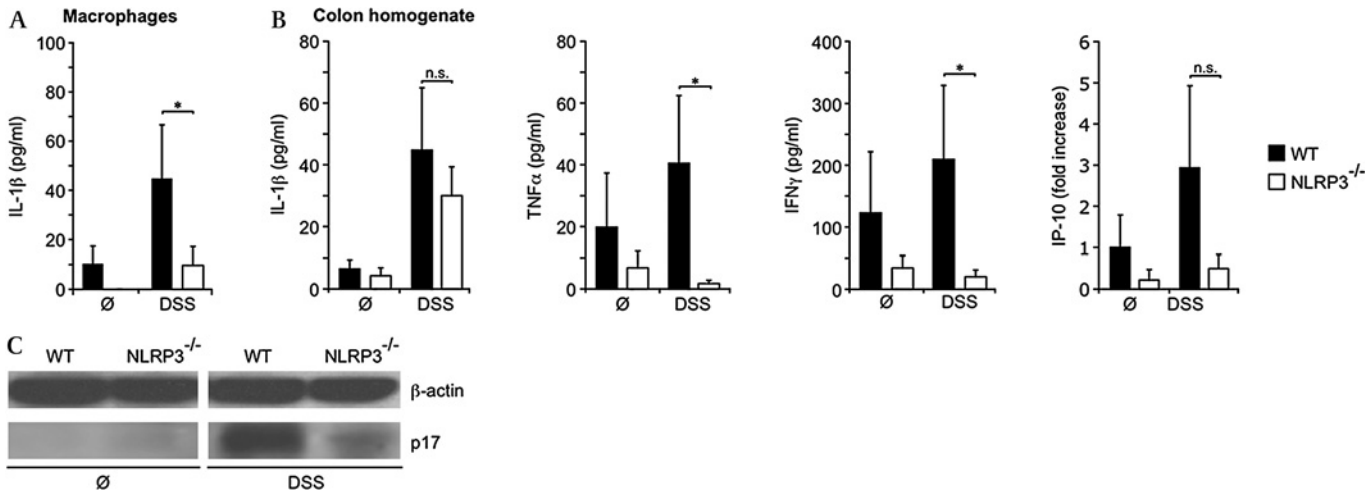

Figure 5 Reduced inflammatory responses in NLRP3$^{-/-}$ mice in response to dextran sodium sulfate (DSS). (A) Peritoneal macrophages of wild-type (WT) and NLRP3$^{-/-}$ mice (n=5 per group) treated with 2% DSS for 9 days or with tap water were obtained by lavage, and spontaneous release of interleukin 1β (IL-1β) was determined in culture supernatant by ELISA. (B) Cytokine levels in colonic homogenate of WT and NLRP3$^{-/-}$ mice. Levels of IL-1β, tumour necrosis factor α (TNFα) and interferon γ (IFNγ) were analysed by ELISA. IP-10 expression was assessed by quantitative reverse transcription–PCR. Data are presented as means ± SEM (n=2 independent experiments). *$p<0.05$. (C) Western blots of IL-1β (p17) in colonic homogenate of DSS-treated WT and NLRP3$^{-/-}$ mice.

DISCUSSION

Data from human specimens and from murine colitis models indicate that excessive expression of IL-1β and IL-18 plays a key role in the pathogenesis of IBD.[5 31] Furthermore, caspase-1, which regulates the secretion of biologically active IL-1β and IL-18, has been identified as a central mediator of DSS-induced colitis.[9] In the present study, we provide evidence that DSS induces caspase-1 activation via the NLRP3 inflammasome in macrophages and that NLRP3$^{-/-}$ mice are significantly protected from DSS-induced colitis, developing a decreased clinical and histological colitis severity and dramatically reduced levels of proinflammatory cytokines in the colonic tissue. This protective effect was most pronounced at an early time point of the disease, indicating a critical role for the NLRP3 inflammasome at the initiation of the inflammatory process. Together, these results strongly argue for a role for the NLRP3 inflammasome in DSS-induced colitis. Interestingly, the clinical colitis severity parameters in NLRP3$^{-/-}$ mice were comparable with those achieved by inhibition of caspase-1 with pralnacasan in WT mice, indicating that pharmacological intervention in the NLRP3 inflammasome complex may have therapeutic potential in the treatment of IBD.[23]

The precise mechanism of NLRP3 inflammasome activation is incompletely understood. The data obtained in the present study demonstrate that IL-1β release by macrophages in response to DSS requires lysosomal maturation, the lysosomal proteases cathepsin B and cathepsin L, loss of lysosomal integrity as well as ROS production. These mechanisms resemble those previously described for other NLRP3 stimuli, such as monosodium urate, asbestos, silica crystals and influenza virus.[21 28 29] Assays measuring IL-1β production by DSS-stimulated macrophages could be exploited for high-throughput screening of new anti-inflammatory drugs targeting the NLRP3 inflammasome for the treatment of IBD.

In what respect can these findings contribute to our understanding of human IBD? Genetic studies provide evidence for an association of IBD with mutations of NLRP3 inflammasome components. Villani and co-workers found that susceptibility to Crohn's disease is associated with polymorphisms located in a predicted regulatory region on chromosome 1q44 downstream of NLRP3.[16] Interestingly, these polymorphisms correlated with impairment of IL-1β processing of PBMCs in response to LPS, indicating that NLRP3-mediated caspase-1 activation may play a protective role in IBD, for example in the defence of intestinal microbial pathogens. On the other hand, McGovern and co-workers detected an association between IBD and a polymorphism of CARD8 (C10X),[32] even though this could not be confirmed by others.[33 34] CARD8 is a binding partner of NLRP3 and as such a component of the NLRP3 inflammasome.[35] It is known to suppress NF-κB activity and to regulate caspase-1 activation.[36 37] Similarly to mutations in NOD2, CARD8 mutations might lead to perturbations in the NF-κB pathway, finally leading to upregulation of pro-IL-1β and pro-IL-18 in lamina propria macrophages. In the same model, an additional gain-of-function mutation of NLRP3 could lead to an over-activated caspase-1, cleaving pro-IL-1β and pro-IL-18 into their biologically active forms. In support of this hypothesis, Schoultz and co-workers have recently reported that combined NLRP3 and CARD8 mutations increase the susceptibility to Crohn's disease in a cohort of Swedish men.[17]

This 'two-hit' model of caspase-1 activation leading to the secretion of IL-1β and IL-18 in human IBD appears to be closely mirrored in the DSS colitis model in mice. Initially, DSS exerts a direct toxic effect on the epithelial barrier, hence allowing bacteria to stimulate lamina propria macrophages via TLRs and the NF-κB pathway, which leads to enhanced transcription of pro-IL-1β and pro-IL-18.[38] In a second step, DSS induces caspase-1 activation via the NLRP3 inflammasome complex, cleaving IL-1β and IL-18 into their biologically active forms, which initiates an intestinal inflammatory cascade. Our data may thus help to understand why DSS-induced colitis is, despite its striking simplicity, such a valuable model of IBD.

Acknowledgements We thank Nadja Sandholzer for excellent animal husbandry. This work is part of the PhD thesis of PD and CM at the University of Munich. This work was supported by the Deutsche Krebshilfe (Max Eder Research Grant to MS), the Deutsche Forschungsgemeinschaft (GK 1202) to MS and SE, GK 1202 student grant to PD, and En 169/7-2 to SE.

Competing interests None.

Provenance and peer review Not commissioned; externally peer reviewed.

REFERENCES

1. **Podolsky DK.** Inflammatory bowel disease. *N Engl J Med* 2002;**347**:417—29.
2. **Okayasu I,** Hatakeyama S, Yamada M, *et al*. A novel method in the induction of reliable experimental acute and chronic ulcerative colitis in mice. *Gastroenterology* 1990;**98**:694—702.
3. **Dieleman LA,** Ridwan BU, Tennyson GS, *et al*. Dextran sulfate sodium-induced colitis occurs in severe combined immunodeficient mice. *Gastroenterology* 1994;**107**: 1643—52.
4. **Ishiguro Y.** Mucosal proinflammatory cytokine production correlates with endoscopic activity of ulcerative colitis. *J Gastroenterol* 1999;**34**:66—74.
5. **Monteleone G,** Trapasso F, Parrello T, *et al*. Bioactive IL-18 expression is up-regulated in Crohn's disease. *J Immunol* 1999;**163**:143—7.
6. **Sartor RB.** Cytokines in intestinal inflammation: pathophysiological and clinical considerations. *Gastroenterology* 1994;**106**:533—9.
7. **Al-Sadi RM,** Ma TY. IL-1beta causes an increase in intestinal epithelial tight junction permeability. *J Immunol* 2007;**178**:4641—9.
8. **Kwon KH,** Murakami A, Hayashi R, *et al*. Interleukin-1beta targets interleukin-6 in progressing dextran sulfate sodium-induced experimental colitis. *Biochem Biophys Res Commun* 2005;**337**:647—54.
9. **Siegmund B,** Lehr HA, Fantuzzi G, *et al*. IL-1 beta-converting enzyme (caspase-1) in intestinal inflammation. *Proc Natl Acad Sci USA* 2001;**98**:13249—54.
10. **Fritz JH,** Ferrero RL, Philpott DJ, *et al*. Nod-like proteins in immunity, inflammation and disease. *Nat Immunol* 2006;**7**:1250—7.
11. **Hugot JP,** Chamaillard M, Zouali H, *et al*. Association of NOD2 leucine-rich repeat variants with susceptibility to Crohn's disease. *Nature* 2001;**411**:599—603.
12. **Ogura Y,** Bonen DK, Inohara N, *et al*. A frameshift mutation in NOD2 associated with susceptibility to Crohn's disease. *Nature* 2001;**411**:603—6.
13. **Maeda S,** Hsu LC, Liu H, *et al*. Nod2 mutation in Crohn's disease potentiates NF-kappaB activity and IL-1beta processing. *Science* 2005;**307**:734—8.
14. **van Beelen AJ,** Zelinkova Z, Taanman-Kueter EW, *et al*. Stimulation of the intracellular bacterial sensor NOD2 programs dendritic cells to promote interleukin-17 production in human memory T cells. *Immunity* 2007;**27**:660—9.
15. **Masters SL,** Simon A, Aksentijevich I, *et al*. Horror autoinflammaticus: the molecular pathophysiology of autoinflammatory disease. *Annu Rev Immunol* 2009;**27**:621—68.
16. **Villani AC,** Lemire M, Fortin G, *et al*. Common variants in the NLRP3 region contribute to Crohn's disease susceptibility. *Nat Genet* 2009;**41**:71—6.
17. **Schoultz I,** Verma D, Halfvarsson J, *et al*. Combined polymorphisms in genes encoding the inflammasome components NALP3 and CARD8 confer susceptibility to Crohn's disease in Swedish men. *Am J Gastroenterol* 2009;**104**:1180—8.
18. **Prescott NJ,** Fisher SA, Franke A, *et al*. A nonsynonymous SNP in ATG16L1 predisposes to ileal Crohn's disease and is independent of CARD15 and IBD5. *Gastroenterology* 2007;**132**:1665—71.
19. **Rioux JD,** Xavier RJ, Taylor KD, *et al*. Genome-wide association study identifies new susceptibility loci for Crohn disease and implicates autophagy in disease pathogenesis. *Nat Genet* 2007;**39**:596—604.
20. **Saitoh T,** Fujita N, Jang MH, *et al*. Loss of the autophagy protein Atg16L1 enhances endotoxin-induced IL-1beta production. *Nature* 2008;**456**:264—8.
21. **Hornung V,** Bauernfeind F, Halle A, *et al*. Silica crystals and aluminum salts activate the NALP3 inflammasome through phagosomal destabilization. *Nat Immunol* 2008;**9**:847—56.
22. **Martinon F,** Petrilli V, Mayor A, *et al*. Gout-associated uric acid crystals activate the NALP3 inflammasome. *Nature* 2006;**440**:237—41.
23. **Bauer C,** Loher F, Dauer M, *et al*. The ICE inhibitor pralnacasan prevents DSS-induced colitis in C57BL/6 mice and suppresses IP-10 mRNA but not TNF-alpha mRNA expression. *Dig Dis Sci* 2007;**52**:1642—52.
24. **Martinon F,** Mayor A, Tschopp J. The inflammasomes: guardians of the body. *Annu Rev Immunol* 2009;**27**:229—65.
25. **Petrilli V,** Papin S, Dostert C, *et al*. Activation of the NALP3 inflammasome is triggered by low intracellular potassium concentration. *Cell Death Differ* 2007;**14**: 1583—9.
26. **Fernandes-Alnemri T,** Wu J, Yu JW, *et al*. The pyroptosome: a supramolecular assembly of ASC dimers mediating inflammatory cell death via caspase-1 activation. *Cell Death Differ* 2007;**14**:1590—604.
27. **Mariathasan S,** Weiss DS, Newton K, *et al*. Cryopyrin activates the inflammasome in response to toxins and ATP. *Nature* 2006;**440**:228—32.
28. **Allen IC,** Scull MA, Moore CB, *et al*. The NLRP3 inflammasome mediates in vivo innate immunity to influenza a virus through recognition of viral RNA. *Immunity* 2009;**30**:556—65.
29. **Dostert C,** Petrilli V, Van Bruggen R, *et al*. Innate immune activation through Nalp3 inflammasome sensing of asbestos and silica. *Science* 2008;**320**:674—7.
30. **Kwon KH,** Ohigashi H, Murakami A. Dextran sulfate sodium enhances interleukin-1 beta release via activation of p38 MAPK and ERK1/2 pathways in murine peritoneal macrophages. *Life Sci* 2007;**81**:362—71.
31. **Siegmund B,** Fantuzzi G, Rieder F, *et al*. Neutralization of interleukin-18 reduces severity in murine colitis and intestinal IFN-gamma and TNF-alpha production. *Am J Physiol Regul Integr Comp Physiol* 2001;**281**:R1264—73.
32. **McGovern DP,** Butler H, Ahmad T, *et al*. TUCAN (CARD8) genetic variants and inflammatory bowel disease. *Gastroenterology* 2006;**131**:1190—6.
33. **Fisher SA,** Mirza MM, Onnie CM, *et al*. Combined evidence from three large British Association studies rejects TUCAN/CARD8 as an IBD susceptibility gene. *Gastroenterology* 2007;**132**:2078—80.
34. **Franke A,** Rosenstiel P, Balschun T, *et al*. No association between the TUCAN (CARD8) Cys10Stop mutation and inflammatory bowel disease in a large retrospective German and a clinically well-characterized Norwegian sample. *Gastroenterology* 2007;**132**:2080—1.
35. **Agostini L,** Martinon F, Burns K, *et al*. NALP3 forms an IL-1beta-processing inflammasome with increased activity in Muckle-Wells autoinflammatory disorder. *Immunity* 2004;**20**:319—25.
36. **Bouchier-Hayes L,** Conroy H, Egan H, *et al*. CARDINAL, a novel caspase recruitment domain protein, is an inhibitor of multiple NF-kappa B activation pathways. *J Biol Chem* 2001;**276**:44069—77.
37. **Razmara M,** Srinivasula SM, Wang L, *et al*. CARD-8 protein, a new CARD family member that regulates caspase-1 activation and apoptosis. *J Biol Chem* 2002;**277**: 13952—8.
38. **Fukata M,** Chen A, Vamadevan AS, *et al*. Toll-like receptor-4 promotes the development of colitis-associated colorectal tumors. *Gastroenterology* 2007;**133**: 1869—81.

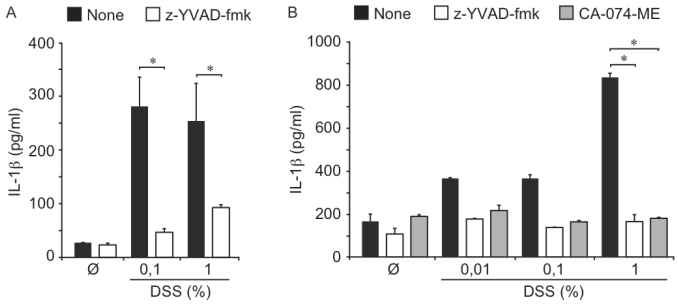
A
None
z-YVAD-fmk
IL-1β (pg/ml)
400
300
200
100
0
*
*
Ø
0,1
1
DSS (%)
B
None
z-YVAD-fmk
CA-074-ME
IL-1β (pg/ml)
1000
800
600
400
200
0
*
*
Ø
0,01
0,1
1
DSS (%)

Suppl. Fig. 1

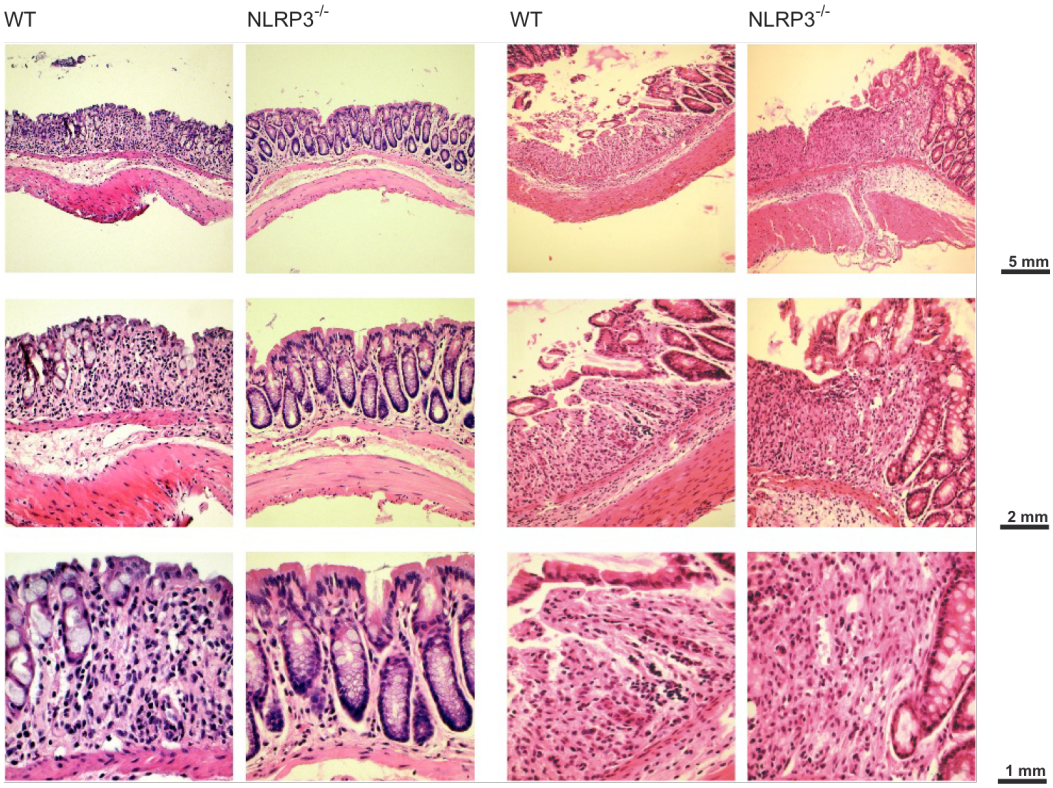

Suppl. Fig. 2

3. Danksagung

Mein Dank gilt insbesondere meinem Doktorvater PD Dr. med. Max Schnurr für das Vertrauen, die Unterstützung und die exzellente Anleitung zum wissenschaftlichen Denken und Handeln.

Bedanken möchte ich mich auch bei Herrn Professor Dr. med. Stefan Endres für die herzliche Aufnahme in die Klinische Pharmakologie, mit allen Kollegen, die für eine außergewöhnliche und angenehme Atmosphäre sorgten.

Für die exzellente Kooperation mit Herrn Professor Dr. med. Eicke Latz an der *University of Massachusetts Medical School* und am Universitätsklinikum Bonn, möchte ich mich ausdrücklich bedanken.

Ebenfalls bedanken möchte ich mich bei meinem Mitbetreuer Dr. rer. biol. hum. Klaus Heckelsmiller und meinen Kollegen in der Arbeitsgruppe, die mit Rat und Tat stets zur Verfügung standen.

Außerdem gilt mein besonderer Dank meinen Eltern Klaus und Petra Düwell und meiner Freundin Barbara Major, für die jahrelange Unterstützung und Geduld, die stets vorhanden waren.

4. Veröffentlichungen

4.1 Originalarbeiten

1. **Peter Duewell***, Hajime Kono*, Katey J. Rayner, Cherilyn M. Sirois, Gregory Vladimer, Franz G. Bauernfeind, George S. Abela, Luigi Franchi, Gabriel Nuñez, Max Schnurr, Terje Espevik, Egil Lien, Katherine A. Fitzgerald, Kenneth L. Rock, Kathryn J. Moore, Samuel D Wright, Veit Hornung* and Eicke Latz*.

   NLRP3 inflammasomes are required for atherogenesis and activated by cholesterol crystals early in disease.

   Nature 2010 Apr 29;464(7293):1357-61.

2. Christian Bauer*, **Peter Duewell***, Christine Mayer, Hans Anton Lehr, Kate A. Fitzgerald, Marc Dauer, Jurg Tschopp, Stefan Endres, Eicke Latz, and Max Schnurr.

   Colitis induced in mice with dextran sulfate sodium (DSS) is mediated by the NLRP3 inflammasome.

   Gut 2010 May 4. doi:10.1136/gut.2009.197822.

3. Collin Jacobs*, **Peter Duewell***, Klaus Heckelsmiller, Jiwu Wei, Franz Bauernfeind, Jonathan Ellermeier, Ulrich Kisser, Christian A. Bauer, Marc Dauer, Andreas Eigler, Eugene Maraskovsky, Stefan Endres, and Max Schnurr.

   An ISCOM vaccine combined with a TLR9 agonist breaks immune evasion mediated by regulatory T cells in an orthotopic model of pancreatic carcinoma.

   Int J Cancer 2010 Apr 19. [Epub ahead of print].

* Contributed equally

4.2 Abstracts

1. Collin Jacobs, Klaus Heckelsmiller, **Peter Düwell**, Franz Bauernfeind, Christian Bauer, Marc Dauer, Andreas Eigler, Stefan Endres, Max Schnurr.

   Vaccination with an ISCOM-based tumor vaccine and a TLR ligand overcomes tumor-induced immune suppression and leads to eradication of pancreatic carcinoma.

   62. Jahrestagung der Deutschen Gesellschaft für Verdauungs- und Stoffwechselkrankheiten, 2007.

2. Max Schnurr, Collin Jacobs, Klaus Heckelsmiller, **Peter Düwell**, Marc Dauer, Andreas Eigler, Eugene Maraskovsky.

   Linking innate and adaptive immunity by vaccination with adjuvant-formulated tumor antigen.

   7th World Congress on Trauma, Shock, Inflammation and Sepsis – TSIS 2007.

3. Max Schnurr, **Peter Düwell**, Collin Jacobs, Jiwu Wei, Marc Dauer, Andreas Eigler, Stefan Endres.

   Durchbrechung der vom Pankreaskarzinom ausgehenden Immunsuppression durch Depletion regulatorischer T- Zellen.

   36. Jahrestagung der Gesellschaft für Gastroenterologie in Bayern, 2008.

4. Max Schnurr, Jiwu Wei, **Peter Düwell**, Collin Jakobs, Marc Dauer, Stefan Endres, Andreas Eigler.

   Die Rolle regulatorischer T-Zellen im murinen Pankreaskarzinom: Herausforderung für die Entwicklung effektiver Immuntherapien.

   63. Jahrestagung der Deutschen Gesellschaft für Verdauungs- und Stoffwechselkrankheiten, 2008.

5. Jonathan Ellermeier, Jiwu Wei, **Peter Düwell**, Stefan Endres, Max Schnurr.

   Treatment of pancreatic carcinoma with a 5'-Triphosphate siRNA targeting the immunosuppressive molecule TGFβ1.

   64. Jahrestagung Deutsche Gesellschaft für Verdauungs- und Stoffwechselkrankheiten, 2009.

6. Jonathan Ellermeier, Jiwu Wei, **Peter Düwell**, Stefan Endres, Max Schnurr.

   Tri-functional siRNA combining TGF-beta silencing, RIG-I activation and apoptosis induction induces effective antitumor responses in pancreatic Carcinoma.

   29. Deutscher Krebskongress, Berlin, 2010.

7. **Peter Duewell**, Christian Bauer, Christine Mayer, Hans Anton Lehr, Katherine A. Fitzgerald, Jurg Tschopp, Stefan Endres, Eicke Latz and Max Schnurr.

   Colitis induced in mice with dextran sulfate sodium (DSS) is mediated by the NLRP3 inflammasome.

   Keystone Symposia. Innate Immunity: Mechanisms Linking with Adaptive Immunity, Trinity College Dublin, 2010.

5. Lebenslauf

Peter Düwell

geboren am 27. Juni 1980 in Oberstdorf im Allgäu als Sohn von Petra und Klaus Düwell.

Bildungsweg

1991 – 2000	Gertrud von le Fort Gymnasium Oberstdorf/Allgäu, Abitur
2001 – 2005	Studium der Pharmazie an der Ludwig-Maximilians-Universität in München
2005 – 2006	Praktisches Jahr. Hexal Pharmaforschung GmbH, Holzkirchen, Forschung und Entwicklung, Abteilung für Strukturaufklärung (1. Halbjahr). Bienenapotheke Parkstadt Schwabing, München (2. Halbjahr)
2006	Approbation als Apotheker

Promotion

2006 – 2010	Doktorarbeit in der Abteilung für Klinische Pharmakologie (Leiter: Prof. Dr. med. Stefan Endres) in der Arbeitsgruppe von PD Dr. med. Max Schnurr, Medizinische Klinik Innenstadt, Klinikum der Universität München
07-2009 – 11-2009	Forschungsaufenthalt in der Arbeitsgruppe von Prof. Eicke Latz, Division of Infectious Diseases & Immunology, University of Massachusetts Medical School, Worcester, USA

Beruf

Seit 2006	Klinisch-Pharmakologischer Konsiliardienst, Abteilung für Klinische Pharmakologie (Prof. Dr. S. Endres)
2006 – 2009	Bereitschaftsdienste in der Bienenapotheke Sendling, München

Seit 2010	Wissenschaftlicher Mitarbeiter in der Medizinischen Klinik Innenstadt der Universität München

Stipendien

2006 – 2009	DFG-Promotionsstipendium im Graduiertenkolleg 1202 "Oligonukleotide in Zellbiologie und Therapie" an der Medizinischen Klinik Innenstadt der Universität München, Bereich Gastroenterologie und Klinische Pharmakologie
2008	Reisestipendium der GlaxoSmithKline Stiftung für einen Forschungsaufenthalt an der University of Massachusetts Medical School, Worcester, USA
2011	Bewilligung des Antrags auf *Anschubförderung für Erstantragstellende* 2011 des Graduiertenkolleg 1202 "Oligonukleotide in Zellbiologie und Therapie"

Auszeichnungen

2000	Buchpreis des Fonds der Chemischen Industrie im Verband der Chemischen Industrie e.V. in Anerkennung als bester Abiturient im Fach Chemie 2000 am Gertrud-von-le-Fort-Gymnasium Oberstdor
2009	Presidential Poster (Co-Autor) Immunotherapy of pancreatic carcinoma with siRNA targeting TGF-β1 *37. Jahrestagung der Gesellschaft für Gastroenterologie in Bayern, 2009*
2010	Presidential Poster (Co-Autor) Die Dextran Sulfat Sodium (DSS)-induzierte Kolitis wird durch das NLRP3-Inflammasom reguliert *38. Jahrestagung der Gesellschaft für Gastroenterologie in Bayern, 2010*
2011	Hugo Wilhelm von Ziemssen Preis für eine herausragende wissenschaftliche Publikation